The Plant Cell, Vol. 15, 347–364, February 2003, www.plantcell.org © 2003 American Society of Plant Biologists

The Arabidopsis *cax1* Mutant Exhibits Impaired Ion Homeostasis, Development, and Hormonal Responses and Reveals Interplay among Vacuolar Transporters

Ning-Hui Cheng,[a] Jon K. Pittman,[a] Bronwyn J. Barkla,[b] Toshiro Shigaki,[a] and Kendal D. Hirschi[a,c,d,1]

[a] United States Department of Agriculture/Agricultural Research Service Children's Nutrition Research Center, Baylor College of Medicine, Houston, Texas 77030

[b] Instituto de Biotecnología, Universidad Nacional Autónoma de México, Colonia Miraval, Cuernavaca, Morelos 62250, Mexico

[c] Department of Human and Molecular Genetics, Baylor College of Medicine, Houston, Texas 77030

[d] Vegetable and Fruit Improvement Center, Texas A&M University, College Station, Texas 77845

The Arabidopsis Ca^{2+}/H^+ transporter CAX1 (Cation Exchanger1) may be an important regulator of intracellular Ca^{2+} levels. Here, we describe the preliminary localization of CAX1 to the tonoplast and the molecular and biochemical characterization of *cax1* mutants. We show that these mutants exhibit a 50% reduction in tonoplast Ca^{2+}/H^+ antiport activity, a 40% reduction in tonoplast V-type H^+-translocating ATPase activity, a 36% increase in tonoplast Ca^{2+}-ATPase activity, and increased expression of the putative vacuolar Ca^{2+}/H^+ antiporters *CAX3* and *CAX4*. Enhanced growth was displayed by the *cax1* lines under Mn^{2+} and Mg^{2+} stress conditions. The mutants exhibited altered plant development, perturbed hormone sensitivities, and altered expression of an auxin-regulated promoter-reporter gene fusion. We propose that CAX1 regulates myriad plant processes and discuss the observed phenotypes with regard to the compensatory alterations in other transporters.

INTRODUCTION

As in all eukaryotic systems, plant Ca^{2+} signaling depends on the regulation of cytosolic Ca^{2+} levels. For secondary transporters, animals predominately use Na^+ as the coupling ion to circulate Ca^{2+} across biological membranes, whereas plants use protons as the coupling ion almost exclusively (Sze et al., 1999; Gaxiola et al., 2002). Proton gradients are generated by primary H^+-translocating pumps that hydrolyze either ATP (plasma membrane P-type H^+-translocating ATPase and tonoplast V-type H^+-translocating ATPase [V-ATPase]) or PPi (tonoplast H^+-translocating pyrophosphatase [V-PPase]) as the energy source to pump protons, generating a proton motive force that energizes the membrane (Drozdowicz and Rea, 2001; Palmgren, 2001; Sze et al., 2002). Thus, plants use the proton motive force to directly and indirectly regulate the transport of ions such as Ca^{2+} across membranes.

The design and architecture of the plant cell contribute spatial features to the Ca^{2+} spike not seen in mammalian systems, particularly the Ca^{2+} spikes around the vacuole. The plant vacuole can occupy up to 99% of a plant cell's volume (Marty, 1999) and contains various Ca^{2+} channels, including Ca^{2+}-permeable inositol 1,4,5-trisphosphate– and cyclic ADP-ribose–activated channels (Schumaker and Sze, 1987; Allen et al., 1995). These types of channels on the tonoplast suggest that localized Ca^{2+} spikes around the plant vacuole play a pivotal role in determining signal specificity. Furthermore, these findings imply that vacuolar Ca^{2+}/H^+ antiporters driven by the V-ATPase or V-PPase and Ca^{2+}-ATPases help reset cytosolic Ca^{2+} levels after signal transduction. However, there is a paucity of mutants in plant vacuolar Ca^{2+} transporters that can be used to assess the biological impact of these transporters in plant signaling (Wu et al., 2002).

Initially, plant Ca^{2+}/H^+ antiporter genes were cloned by their ability to suppress the Ca^{2+}-hypersensitive phenotype of a *Saccharomyces cerevisiae* mutant (Hirschi et al., 1996; Ueoka-Nakanishi et al., 2000). These genes are termed cation exchangers (CAX). CAX1 from Arabidopsis is a high-capacity Ca^{2+} transporter, whereas CAX2 has a lower capacity for Ca^{2+} transport (Hirschi et al., 1996) and also can transport other metals (Hirschi et al., 2000). Arabidopsis appears to have up to 10 other putative cation/H^+ antiporters

[1] To whom correspondence should be addressed. E-mail kendalh@bcm.tmc.edu; fax 713-798-7078.

Article, publication date, and citation information can be found at www.plantcell.org/cgi/doi/10.1105/tpc.007385.

(CAX3 to CAX11 and MHX) (Mäser et al., 2001). Some of these, such as CAX2, CAX4, and MHX, have been shown to localize to the plant vacuole (Shaul et al., 1999; Hirschi et al., 2000; Cheng et al., 2002). Understanding the intracellular localization and function of these individual CAX transporters is an important component of understanding the specificity of Ca^{2+} signals.

The activity of CAX1 appears to be regulated by an N-terminal regulatory region (NRR) that was absent from the initial clone characterized by heterologous expression in yeast (Pittman and Hirschi, 2001; Pittman et al., 2002). Ectopic expression of deregulated CAX1 (termed sCAX1, missing the N-terminal autoinhibitor) in tobacco increases Ca^{2+} levels in the plants and causes numerous stress-sensitive phenotypes often associated with Ca^{2+} deficiencies (Hirschi, 1999, 2001). Thus, a wide range of environmental responses appear to require the judicious control of CAX1 transport activity; however, these studies have not addressed the phenotypic consequences of diminishing Ca^{2+}/H^{+} transport around the plant vacuole.

In this study, we tentatively localize CAX1 in Arabidopsis and demonstrate that in planta CAX1 contains the N-terminal autoinhibitory domain. We report the isolation of *CAX1* knockout mutants and describe the phenotypes of these plants at the whole-plant, molecular, and biochemical levels. Characterization of the mutant phenotypes indicates that the *cax1* disruption alters the expression and/or activity of other vacuolar Ca^{2+} transporters and the V-ATPase. Despite these compensatory changes, *cax1* mutants exhibit alterations in growth, stress responses, and hormone perception. These findings offer a clue to the elaborate regulatory interplay among transporters and suggest that CAX1 transport mediates numerous biological responses.

RESULTS

CAX1 Localizes to the Vacuolar Membrane in Arabidopsis

The localization of CAX1 has not been reported. Previous findings suggest that CAX1 localizes to the vacuolar membrane. First, deregulated N-terminal truncations of CAX1 can suppress yeast mutants defective in vacuolar Ca^{2+} transport (Hirschi et al., 1996); second, when expressed heterologously in yeast, epitope-tagged, full-length, and truncated CAX1 localize to the vacuolar membrane (Pittman and Hirschi, 2001); and third, ectopic expression of deregulated CAX1 increases Ca^{2+}/H^{+} transport in tobacco tonoplast-enriched fractions (Hirschi, 1999). To further establish the subcellular localization of CAX1 in plants, microsomal membranes from wild-type and transgenic lines harboring the hemagglutinin (HA)-tagged truncated CAX1 fusion protein (HA-sCAX1) were fractionated. Centrifugation through a continuous Suc gradient was first used to compare the distribution of the epitope-tagged transporter in both Arabidopsis (Figure 1A) and tobacco BY-2 (Figure 1B) suspension cells and the native full-length CAX1 (Figure 1A) with that of markers for the vacuole, plasma membrane, and endoplasmic reticulum. As shown in Figure 1, when membrane fractions were assayed for CAX1 and HA-sCAX1 accumulation, proteins of ~50 kD increased at ~30% Suc (most abundant in fractions corresponding to 28 and 37% Suc, respectively). Both endogenous CAX1 and HA-sCAX1 accumulated in fractions enriched in vacuolar membranes, as indicated by the sedimentation profiles, which overlap with that of a resident protein (V-PPase) from this membrane. Furthermore, the profile of the protein detected by anti-CAX1 was unchanged in gradients prepared in the presence of Mg^{2+}, whereas the endoplasmic reticulum, as detected by anti-BiP, showed a large characteristic Mg^{2+} shift to heavier density fractions (Figure 1A).

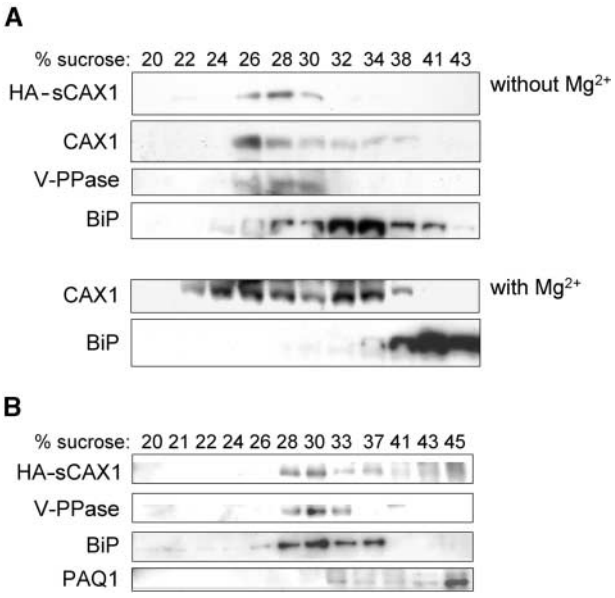

Figure 1. Subcellular Localization of CAX1 in Arabidopsis.

Immunoblot analysis of CAX1 in Arabidopsis **(A)** and tobacco BY-2 cells **(B)**. Equal amounts of protein (10 μg) isolated from HA-sCAX1–expressing transgenic Arabidopsis, wild-type Arabidopsis, and HA-sCAX1–expressing tobacco BY-2 cells were separated by SDS-PAGE, blotted, and subjected to protein gel blot analysis using antibodies against HA (HA-sCAX1), an N-terminal peptide from full-length CAX1 (CAX1), and plant membrane markers: the plant endoplasmic reticulum luminal protein (BiP), mung bean vacuolar pyrophosphatase (V-PPase), and radish plasma membrane aquaporin (PAQ1). Wild-type Arabidopsis membranes were prepared and fractionated in the absence or presence of 5 mM $MgCl_2$, as indicated in **(A)**, and then assayed for changes in CAX1 and BiP expression. Numbers above the gels indicate the Suc concentration of each fraction.

Isolation of *CAX1* Knockout Mutants

Insertional mutagenesis is a means of disrupting gene function based on the insertion of foreign DNA, either transposable elements or T-DNA, into the gene of interest (McKinney et al., 1995; Krysan et al., 1996). Although the insertions are random in nature, it is possible to generate a large number of these insertions; thus, there is a high probability of obtaining an insert in the gene of interest. Collections of insertional mutant lines are now available for which the insertion site has been sequenced and the information deposited into databases (Barbier-Brygoo et al., 2001). This information allows the identification of mutants and helps compensate for the inability to perform efficient targeted disruptions in Arabidopsis. To investigate the physiological function of CAX1 in plants, we used PCR to screen a large population of transposon insertion lines from two different sources (Parinov et al., 1999; Tissier et al., 1999).

We screened a large population of d*Spm* insertion lines from the SLAT pools (Sainsbury Laboratory *Arabidopsis thaliana* Transposants) (Tissier et al., 1999). As shown in Figure 2A, we isolated an Arabidopsis plant of the Columbia ecotype (Col-0) carrying a d*Spm* insertion within the CAX1 open reading frame located in the acidic motif of CAX1, between Gln-266 and Glu-267 (*cax1-1*). The d*Spm* insertion confers BASTA resistance. A homozygous line was isolated by PCR analysis combined with BASTA selection. We also used a SGT (Singapore Gene Trap) *Ds* transposon insertion pool (Parinov et al., 1999) to isolate another allele, *cax1-2*, in the Landsberg *erecta* (L*er*) ecotype. This *Ds* insertion conferred kanamycin resistance; 15 plants from this line contained the proper diagnostic PCR products. Homozygous lines were identified by PCR combined with kanamycin selection. Sequence analysis of the junction of the *Ds* insert determined that it was located between Ala-313 and Ser-314, which is between putative transmembrane spans 7 and 8 in the CAX1 coding sequence (Figure 2A). These disruptions in *CAX1* did not produce detectable levels of *CAX1* RNA (Figure 2B) even when high levels (10 mM) of exogenous Ca^{2+} were added, an environmental factor that increases the levels of *CAX1* RNA significantly (Hirschi, 1999). In addition, neither allele produced detectable levels of CAX1 protein (Figure 2C and data not shown), whereas both alleles of *cax1* were fertile.

Both the *cax1-1* and *cax1-2* alleles were backcrossed to the wild type, and the F1 and F2 progeny were analyzed. The F2 progeny segregated 3:1 for the antibiotic resistance (378 BASTA-resistant seedlings:128 BASTA-sensitive seedlings for *cax1-1* and 205 kanamycin-resistant seedlings:71 kanamycin-sensitive seedlings for *cax1-2*), indicating that both alleles contain a single transposon insertion with a functional selection marker.

To remove any possibility that the *cax1* phenotypes were caused by an unknown mutation, it was important to express *CAX1* in the mutants to restore CAX1-mediated Ca^{2+}/H^{+} antiport activity. For these comparisons, we generated 15 transgenic lines (*cax1-1*:*CAX1*) harboring the cDNA encoding deregulated CAX1 (sCAX1) under the control of the 35S promoter of *Cauliflower mosaic virus* (Hirschi, 1999). The *cax1-1* lines expressing deregulated *CAX1* contained high levels of *CAX1* RNA and CAX1 protein (Figure 2B and data not shown).

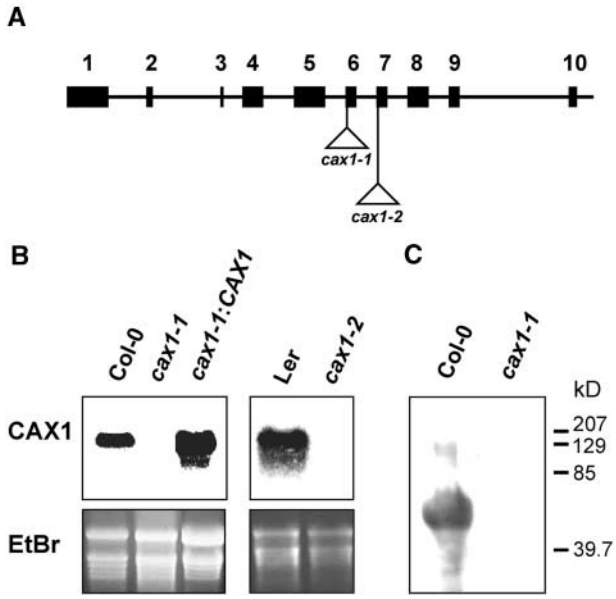

Figure 2. Identification of Transposon Insertion Lines of *CAX1*.

(A) Diagram of the genomic *CAX1* DNA depicting the sites of transposon insertions. The 4.1 kb of genomic *CAX1* DNA is represented by 9 introns (lines) and 10 exons (boxes). Triangles depict the sites of the transposon insertions. The lines harboring these insertions are termed *cax1-1* and *cax1-2*.

(B) RNA gel blot analysis of *CAX1* gene expression in wild-type and *cax1* plants. Total RNA was extracted from 3-week-old wild-type, *cax1* mutant, and *CAX1*-expressing *cax1* plants pretreated with 10 mM $CaCl_2$ overnight. Ten micrograms of total RNA of each sample was loaded, blotted, and hybridized with a ^{32}P-labeled *CAX1* cDNA probe. Ethidium bromide (EtBr) staining of the agarose gel is shown as a loading control.

(C) Immunoblot analysis of CAX1 protein expression in wild-type and *cax1-1* mutant plants pretreated with 100 mM $CaCl_2$ overnight. Twenty micrograms of vacuole-enriched protein sample was separated by SDS-PAGE, blotted, and subjected to protein gel blot analysis using a CAX1-specific antibody.

V-ATPase Activity Is Altered in the *cax1* Mutants

The H^{+} driving force for CAX1 Ca^{2+}/H^{+} antiport activity on the tonoplast is provided by primary H^{+} pumps that coreside on this membrane and acidify the vacuolar lumen. ATP- and PPi-dependent H^{+} transport, as determinants of

V-ATPase and V-PPase activities, respectively, were measured in tonoplast vesicles from Col-0, *cax1-1*, *cax1-1*:*CAX1*, L*er*, and *cax1-2*. V-ATPase H^+ transport activity, determined in the absence of Ca^{2+} in the reaction buffer, was reduced significantly in the *cax1* mutant plants: by 38% in *cax1-1* and by 45% in *cax1-2* compared with the wild type (Figure 3). This reduction in V-ATPase activity in *cax1* was independent of pretreatment of the plants with Ca^{2+} before harvest (data not shown). V-ATPase activity also was measured in *cax1-1* expressing deregulated *CAX1*. These plants showed a 26% increase in H^+ transport activity compared with Col-0 plants (Figure 3). By contrast, V-PPase activity was negligible in roots of Col-0 plants, and no change was detected in *cax1* mutants or *cax1-1* expressing deregulated *CAX1* (data not shown). Furthermore, a preliminary examination of *cax1-1* vacuolar morphology suggested no alterations in vacuolar size or shape compared with wild-type plants (data not shown).

cax1-1 Mutants Display Altered Vacuolar Ca^{2+} Transport

We demonstrated previously that Ca^{2+}/H^+ antiport activity can be measured directly in vacuole-enriched membrane vesicles isolated from Arabidopsis after pretreatment of the plants with 100 mM $CaCl_2$, whereas without high Ca^{2+} induction, Ca^{2+}/H^+ antiport activity is difficult to measure (Pittman et al., 2002). Increased expression of *CAX1* mRNA is observed in the presence of exogenous Ca^{2+}, and we believe that the Ca^{2+}/H^+ antiport activity observed in the Ca^{2+}-treated plants is predominantly the result of CAX1, because this activity is inhibited significantly by a CAX1-specific synthetic peptide (Pittman et al., 2002). To confirm that the loss of the *CAX1* transcript in *cax1-1* mutants caused the disruption of Ca^{2+}/H^+ antiport activity, root tissue was harvested from 4-week-old plants that were pretreated with 100 mM Ca^{2+} 18 h before harvest. Although significant Ca^{2+}/H^+ antiport activity was observed in vesicles from wild-type Col-0 plants, antiport activity in vesicles from *cax1-1* plants was reduced by >50% (Figure 4A).

The vacuolar membrane of Arabidopsis possesses a type-IIB Ca^{2+}-ATPase, ACA4, that is regulated by calmodulin (Geisler et al., 2000). Ca^{2+} uptake into the vacuole-enriched vesicles from both Col-0 and *cax1-1* was measured in the absence of vanadate to determine Ca^{2+}-ATPase activity. In the absence of calmodulin, very little Ca^{2+}-ATPase activity was measured (data not shown). However, in the presence of calmodulin, Ca^{2+}-ATPase activity was high in vesicles from both plants but was significantly higher in vesicles from *cax1-1* compared with Col-0 (Figure 4B), indicating a 36% increase in Ca^{2+}-ATPase activity in plants lacking *CAX1*.

Ca^{2+} transport activity was compared in vacuole-enriched vesicles from Col-0 and *cax1-1* expressing deregulated *CAX1*. Without the addition of exogenous Ca^{2+}, a significant increase in Ca^{2+}/H^+ antiport activity was measured in vesicles from the deregulated *CAX1*-expressing Arabidopsis compared with those from Col-0, whereas no change in Ca^{2+}-ATPase activity was observed (data not shown).

Ca^{2+}/H^+ antiport activity also was measured in vesicles from Col-0 and *cax1-1* in the presence of the CAX1-NRR peptide. As demonstrated previously, in the presence of the CAX1-NRR peptide, Ca^{2+}/H^+ antiport activity from wild-type plants was reduced significantly (Figure 4C). However, there was no difference in antiport activity in vesicles from *cax1-1* roots in the presence or absence of the CAX1-NRR peptide. Furthermore, the CAX1-NRR peptide had no effect on Ca^{2+}-ATPase activity in either Col-0 or *cax1-1* membrane vesicles (data not shown).

Putative Vacuolar Ca^{2+} Transporters Are Upregulated in the *cax1* Mutants

Because of the alterations in vacuolar Ca^{2+}/H^+ antiport, Ca^{2+}-ATPase, and V-ATPase activity, we hypothesized that transporter genes that may be responsive to alterations in Ca^{2+} levels would be deregulated in the mutants. *CAX3* RNA increases when exogenous Ca^{2+} and Na^+ are in the medium but is expressed normally at relatively low levels (Shigaki and Hirschi, 2000). Under nonstressed conditions, *CAX4* RNA can be detected only by reverse transcriptase–

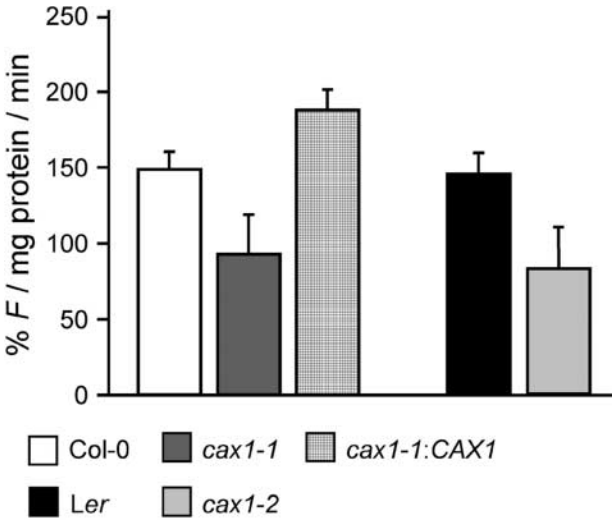

Figure 3. Initial Rates of V-ATPase H^+ Transport Activity in Purified Tonoplast Vesicles from the Wild Type, *cax1*, and *cax1-1* Expressing *CAX1*.

ATP-dependent H^+ transport into tonoplast vesicles (vesicle acidification) was monitored by the quenching of quinacrine fluorescence. Initial rates were calculated from the rates of quinacrine fluorescence quenching during the first 40 s after the addition of ATP. Results are means ± SE of three independent membrane preparations. *F*, fluorescence intensity.

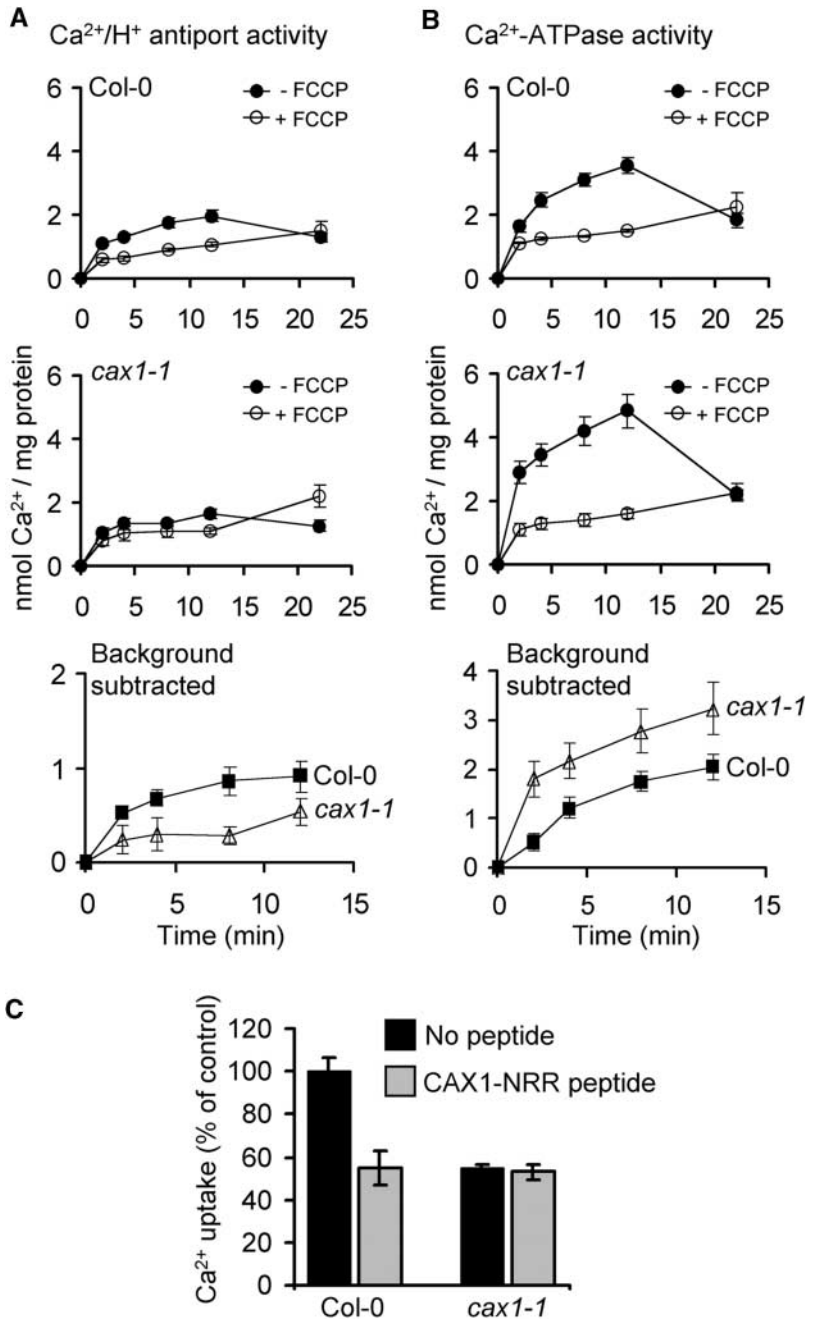

Figure 4. Ca^{2+} Uptake Activity into Vacuole-Enriched Membrane Vesicles from Ca^{2+}-Treated Col-0 and *cax1-1* Root Tissue.

Time courses of Mg^{2+}-ATP–energized 10 μM $^{45}Ca^{2+}$ uptake were determined in the presence of 0.1 mM NaN_3, 10 mM KCl, 1 mM ATP, and 1 mM $MgSO_4$. ΔpH-dependent Ca^{2+}/H^{+} antiport activity **(A)** was determined in the presence of 0.2 mM orthovanadate (Ca^{2+}-ATPase inhibitor) as the difference between Ca^{2+} uptake in the absence and presence of 5 μM carbonyl cyanide *p*-(trifluoromethoxy)phenylhydrazone (FCCP) (protonophore). Calmodulin-stimulated Ca^{2+}-ATPase activity **(B)** was determined in the absence of orthovanadate and the presence of 0.5 μM calmodulin and 5 μM FCCP. The Ca^{2+} ionophore A23187 (5 μM) was added at the 12-min time point and significantly dissipated Ca^{2+} accumulation mediated by Ca^{2+}/H^{+} antiport or Ca^{2+}-ATPase when measured at the 22-min time point. The results of net Ca^{2+}/H^{+} antiport activity (bottom graph in **[A]**) and Ca^{2+}-ATPase activity (bottom graph in **[B]**) also are shown after the subtraction of the +FCCP background values for the first four time points of active Ca^{2+} accumulation. **(C)** shows ΔpH-dependent 10 μM Ca^{2+} uptake into vacuole-enriched membrane vesicles isolated from Ca^{2+}-treated Col-0 or *cax1-1* Arabidopsis root tissue measured in the presence or absence of 10 μM CAX1-NRR peptide at the 10-min time point. The results shown are percentages of Ca^{2+} uptake of the control sample (absence of peptide) after the subtraction of the FCCP background values. All results are means ± SE of experiments from three to six independent membrane preparations.

mediated PCR, and this gene is induced modestly by salt stress (Cheng et al., 2002). *ACA4*, which encodes a vacuolar Ca^{2+}-ATPase, also is expressed at relatively low levels, and reverse transcriptase–mediated PCR shows a modest induction during salt stress (Geisler et al., 2000). Figure 5A shows that *CAX3*, *CAX4*, and *ACA4* levels were significantly higher in *cax1-1* than in both control plants and *cax1-1* lines expressing deregulated *CAX1*. Specifically, *CAX3* RNA levels increased fourfold, *CAX4* RNA levels increased threefold, and *ACA4* RNA levels increased twofold in *cax1-1* compared with wild-type plants. Na^+ treatment highly upregulated *CAX3* in all plant backgrounds (12-, 14-, and 25-fold in wild-type, *cax1-1*, and *CAX1*-expressing mutant plants, respectively) (Figure 5B). Na^+ treatment also produced an eightfold higher level of *CAX4* RNA and a threefold higher level of *ACA4* in *cax1-1* compared with wild-type plants. Similar increases in the expression of *ACA4* and *CAX3* were seen upon Ca^{2+} treatment in *cax1-1* compared with the wild type (data not shown). Comparable changes in *CAX3*, *CAX4*, and *ACA4* transcripts also were seen in the *cax1-2* allele (data not shown). In all cases, the increased expression of these transporters in *cax1-1* was attenuated by the ectopic expression of deregulated CAX1. The RNA levels of the vacuolar metal/H^+ antiporter *CAX2* (Hirschi et al., 2000), the Na^+/H^+ antiporter *AtNHX1* (Gaxiola et al., 1999), and *FKBP15*, a Ca^{2+} modulator protein (Luan et al., 1996), were not altered significantly during any stress treatment in *cax1-1* and *cax1-2* (Figures 5A and 5B and data not shown).

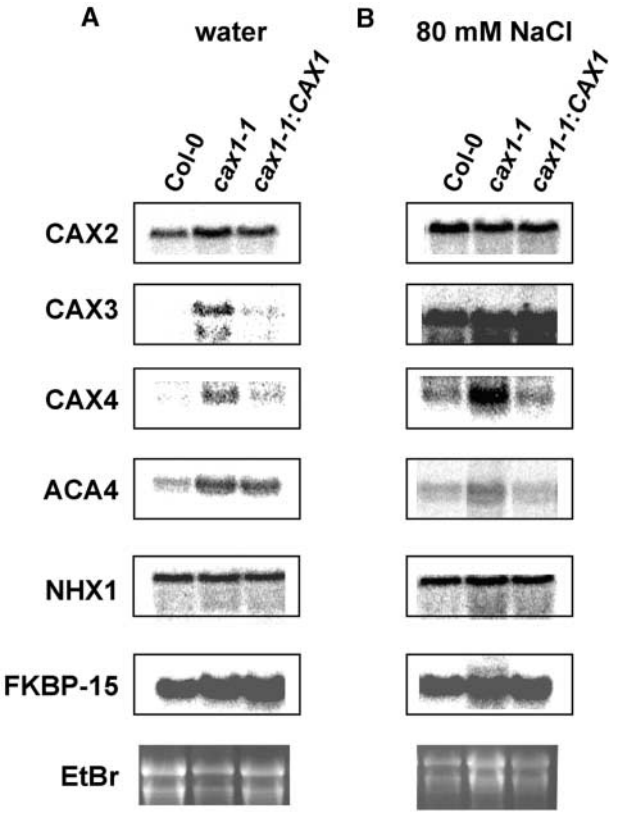

Figure 5. RNA Gel Blot Analysis of Various Transporters.

mRNA expression of various genes in *cax1* mutant plants was analyzed under normal **(A)** and Na^+ stress **(B)** conditions. Total RNA was extracted from 3-week-old wild-type, *cax1* mutant, and *CAX1*-expressing *cax1* plants pretreated with water or 80 mM NaCl overnight. Ten micrograms of total RNA from each sample was loaded, blotted, and hybridized with ^{32}P-labeled DNA probes corresponding to CAX2, CAX3, CAX4, ACA4, NHX1, and FKBP-15. Ethidium bromide (EtBr) staining of the agarose gel is shown as a loading control.

Perturbation of Ion Homeostasis in *cax1* Mutant Plants

Ectopic expression of deregulated *CAX1* increases Ca^{2+} content in transgenic tobacco plants (Hirschi, 1999). However, high-level *CAX1* expression in tobacco causes numerous stress sensitivities associated with Ca^{2+} deficiencies. Although direct measurements of cytosolic Ca^{2+} levels have not been made in these *CAX1*-expressing plants, one hypothesis consistent with these phenotypes is that the sequestration of Ca^{2+} into the vacuole is highly upregulated and Ca^{2+} is "locked" inside the vacuole so that cytosolic Ca^{2+} levels are extremely low, thereby perturbing many Ca^{2+}-dependent processes. To investigate the potential effects of increasing cytosolic Ca^{2+} levels by reducing vacuolar Ca^{2+} sequestration, we examined the ion content and stress sensitivities of *CAX1*–deficient lines.

When *cax1-1* and *cax1-2* were grown in either standard medium or medium containing high levels of Ca^{2+}, there were no measurable changes in the levels of 29 different elements as measured by inductively coupled plasma atomic emission spectrometry (data not shown). This analysis suggested that the disruption of CAX1-mediated Ca^{2+}/H^+ exchange did not alter the total ion content of the plants significantly.

We examined the sensitivity of *cax1* to a variety of different ion perturbations. Both alleles grew in a manner similar to wild-type plants on normal medium (Figures 6A and 6B) and medium containing Li^+, Cd^{2+}, Zn^{2+}, Ni^{2+}, and mannitol (data not shown); however, both *cax1* alleles were more tolerant of Mg^{2+} and Mn^{2+} stresses than wild-type plants (Figures 6C to 6F). In addition, the *cax1* alleles were more tolerant of medium lacking Ca^{2+} (Figures 6G and 6H) and medium containing increased levels of K^+ and Na^+ (data not shown). The ion sensitivities in the wild-type lines could be suppressed to levels similar to those in the *cax1* alleles by the addition of exogenous Ca^{2+} to the growth medium (data not shown). The stress tolerances of the *cax1-1* allele also could be suppressed by the expression of deregulated *CAX1* (data not shown).

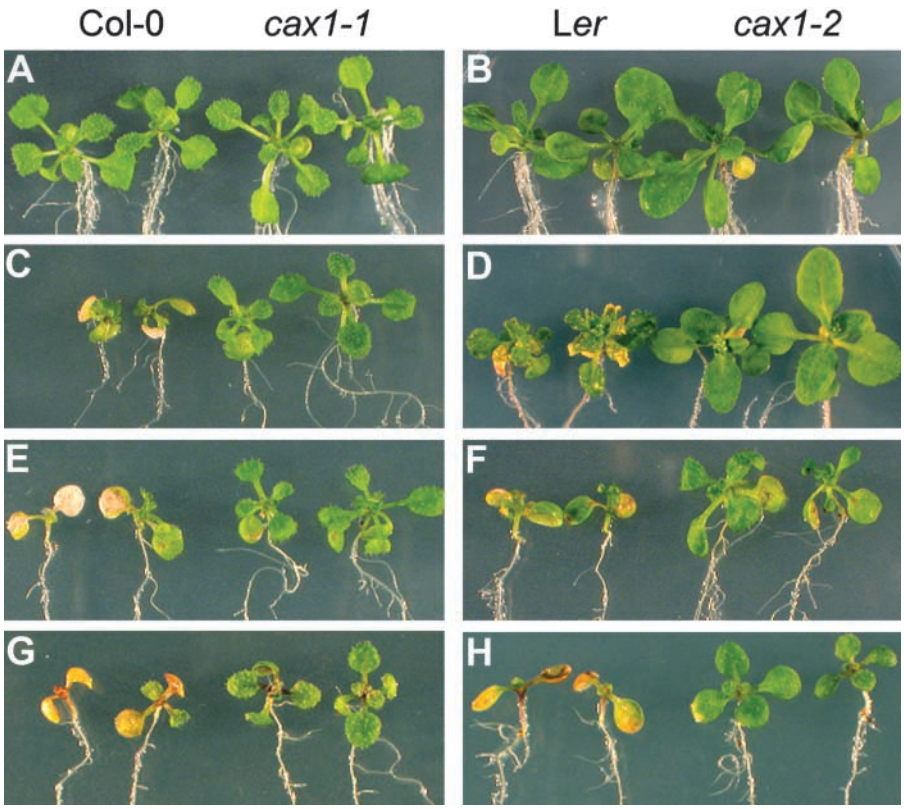

Figure 6. Ion Sensitivity of *cax1* Alleles.

Wild-type (Col-0) and *cax1-1* plants are shown in **(A)**, **(C)**, **(E)**, and **(G)**. Wild-type (L*er*) and *cax1-2* plants are shown in **(B)**, **(D)**, **(F)**, and **(H)**. In each panel, the two wild-type plants are shown at left and the *cax1* plants are shown at right. All photographs are representative of >100 plants grown in each condition.

(A) and **(B)** Five-day-old plants transferred to half-strength MS medium (Murashige and Skoog, 1962) and grown for 5 days.

(C) and **(D)** Five-day-old plants transferred to half-strength MS medium supplemented with 25 mM $MgCl_2$ **(C)** or 10 mM $MgCl_2$ **(D)** and grown for 5 days.

(E) and **(F)** Five-day-old plants transferred to half-strength MS medium supplemented with 1.5 mM $MnCl_2$ and grown for 5 days.

(G) and **(H)** Five-day-old plants transferred to half-strength MS medium without Ca^{2+} and grown for 5 days.

Morphological Phenotypes of *cax1* Alleles

There were no differences in germination time and germination rate observable between the wild-type and the *cax1-1* and *cax1-2* lines (data not shown). The *cax1-1* and *cax1-2* seedlings displayed an ~11% reduction in primary root length when grown on normal medium (Figure 7A). The number of lateral roots was reduced by 25% in *cax1-1*, and there was a 10% reduction in *cax1-2* lateral root number (Figure 7B). Furthermore, the length of the lateral roots was reduced by almost 50% in *cax1-1* and by ~20% in *cax1-2* (Figure 7C).

Under continuous light in soil, the transition of the *cax1-1* and *cax1-2* plants from the vegetative phase to the flowering phase was delayed by ~5 to 7 days (Figure 8). At 27 days, the length of the primary inflorescence stem of *cax1* plants was reduced by ~70% in the *cax1-1* line and by 40% in *cax1-2* (Figure 8B). The number of branching shoots and the total length of the secondary shoots also were reduced significantly in both alleles. The *cax1-1* and *cax1-2* lines were reduced by 58 and 36%, respectively, in the total length of the secondary branches and by 20 and 23%, respectively, in the number of branches (Figures 8D and 8E). The expression of deregulated *CAX1* in the *cax1-1* line suppressed all of these phenotypes (Figure 8).

The alterations in lateral root growth and apical dominance in the *cax1* alleles suggest that auxin levels might be altered in these plants. Given the complex interacting network of hormone response pathways, we analyzed *cax1-1* and *cax1-2* on numerous phytohormones. As shown in Figure 9, the *cax1* roots were resistant to auxin but were tolerant to 1-aminocycloproprane-1-carboxylic acid (an ethylene

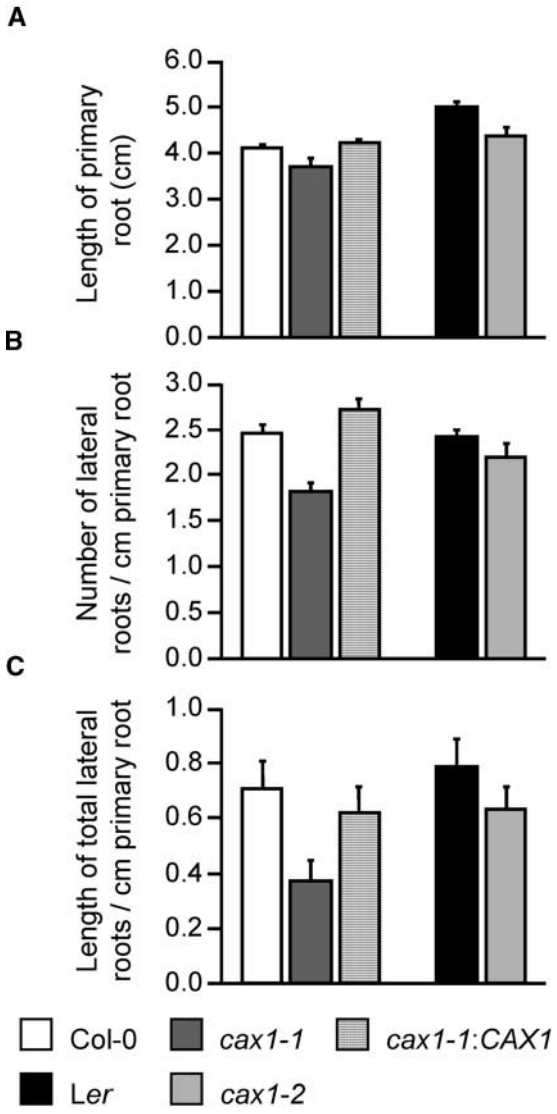

Figure 7. Root Growth Measurements.

Primary roots **(A)** and lateral roots **(B)** and **(C)** of seedlings grown on the same plates at 22°C under continuous light were measured and counted after 10 days of growth on half-strength MS medium. All results are means ± SE ($n \geq 12$). These data are representative of four independent experiments.

precursor), abscisic acid, and benzyladenine (data not shown). This was apparent in the modest resistance to the inhibition of root elongation by exogenous phytohormones. In these conditions, *cax1* roots were no longer shorter than wild-type roots. However, the *cax1* alleles were not completely insensitive to these hormones; for example, auxin treatment did cause *cax1* to form more lateral roots (data not shown). The *cax1* alleles remained sensitive to gibberellic acid and epibrassinolide (data not shown). Furthermore, the expression of deregulated *CAX1* in *cax1-1* reduced root length significantly compared with that in *cax1-1* in the presence of all phytohormones tested (Figures 9B and 9C and data not shown).

IAA28 Expression in the *cax1* Mutant

Reporter elements can be used to infer some of the alterations in the *cax1-1* lines that cannot be detected immediately through whole-plant phenotype analysis. A number of well-characterized auxin reporter lines are available with which to dissect the impact of *cax1* on auxin levels (Abel et al., 1995). These reporters may be especially useful, because several lines of evidence have suggested a relationship between Ca^{2+} homeostasis and auxin regulation (Hasenstein and Evans, 1988). The *Aux/Indoleacetic Acid* (*IAA*) gene family member *IAA28* was used to further characterize the *cax1-1* allele. This reporter is expressed preferentially in roots and inflorescence stems and demonstrates developmental and environmental regulation (Rogg et al., 2001). The *IAA28* promoter–β-glucuronidase (GUS) fusion is expressed strongly from the distal root elongation zone to the root-hypocotyl junction, with the most intense staining in the root hair initiation zone. As shown in Figure 10, incubation of seedlings grown under yellow-filtered light with the GUS substrate 5-bromo-4-chloro-3-indolyl-β-D-glucuronic acid resulted in intense root staining. Unlike other characterized *Aux/IAA* genes, the *IAA28* gene is downregulated by exogenous auxin treatment (Figure 10D) (Rogg et al., 2001). In addition, this reporter appeared to be responsive to Ca^{2+} conditions. As shown in Figures 10B and 10C, under yellow-filtered light, this reporter was downregulated by exogenous Ca^{2+} (Figure 10B) and upregulated in the absence of Ca^{2+} (Figure 10C). *IAA28* promoter–GUS activity was reduced significantly in the *cax1-1* mutant background when grown under various conditions (Figures 10E to 10H). When *cax1-1* harboring the *IAA28* promoter–GUS fusion was grown in normal medium under yellow-filtered light, GUS activity was lower than that in wild-type plants containing the reporter (cf. Figures 10A and 10E). Unlike in the wild-type background, the addition of IAA to *cax1-1* had no obvious effect on *IAA28* expression (Figure 10H). Although the expression of *IAA28* in the *cax1-1* background was increased by the removal of Ca^{2+} (Figure 10G) and decreased by the addition of Ca^{2+} (Figure 10F), the levels still were lower than those of similarly treated controls (Figures 10B and 10C).

DISCUSSION

The data presented here offer insight into the biochemical and molecular mechanisms of Ca^{2+} homeostasis in plants. Cytosolic Ca^{2+} levels are controlled in part by a diverse col-

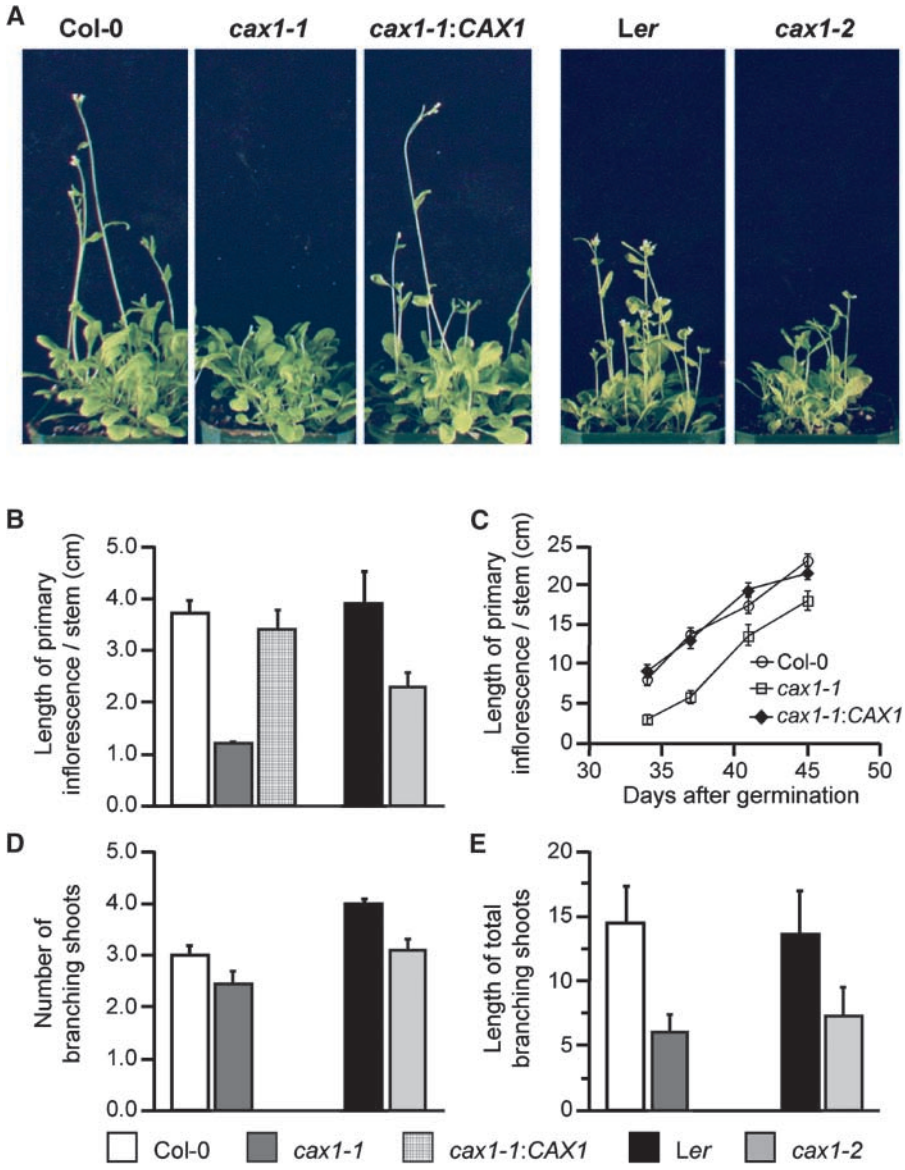

Figure 8. Flowering and Apical Dominance Phenotypes.

(A) Twenty-seven-day-old wild-type and *cax1* plants were grown in soil under continuous light. *cax1* plants are delayed in flowering and shorter in the primary inflorescence stems, and *cax1-1* plants expressing *CAX1* driven by the 35S promoter are indistinguishable from wild-type plants. *cax1-1* and *CAX1*-expressing *cax1-1* are in the Col-0 background, and *cax1-2* is in the L*er* background.

(B) Quantitative analysis of the primary inflorescence stems of 27-day-old wild-type, *cax1*, and *CAX1*-expressing *cax1-1* plants.

(C) Primary inflorescence length of *cax1-1* and wild-type plants over the reproductive phase.

(D) Numbers of branching shoots.

(E) Lengths of branching shoots.

All results are means ± SE ($n \geq 10$). These photographs and data are representative of at least five independent experiments.

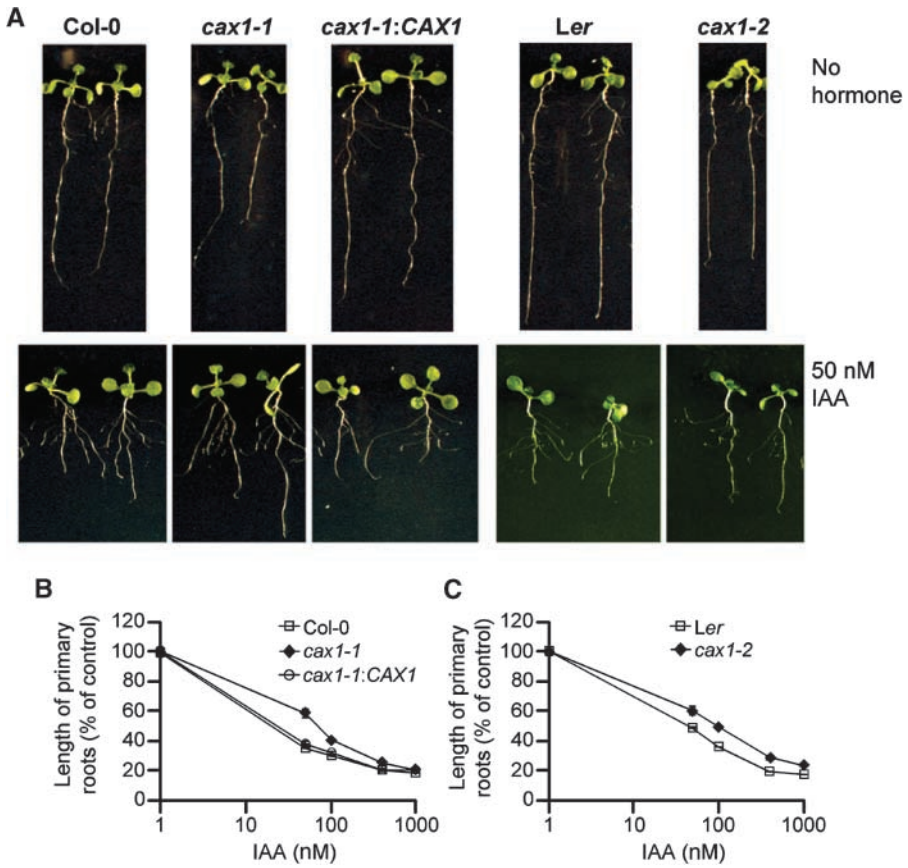

Figure 9. Root Elongation Inhibition by Exogenous Auxin.

(A) *cax1* and wild-type seedlings were germinated and grown on the same plates on standard medium (top row) or standard medium containing 50 nM IAA (bottom row) for 10 days at 22°C under yellow-filtered light.

(B) and **(C)** Quantitative analysis of root elongation inhibition by exogenous auxin. After 10 days of growth under yellow-filtered light on the medium supplemented with various concentrations of IAA, plants were removed from the medium and the lengths of the primary roots were measured. All data are standardized against growth on standard medium. All results are means ± SE ($n \geq 12$). These data are representative of four independent experiments.

lection of Ca^{2+} transporters and channels localized on both the plasma membrane and various internal organelles (Sanders et al., 1999, 2002). The vacuole is the predominant Ca^{2+} store within the cell (Marty, 1999), and both Ca^{2+}-ATPase transporters and Ca^{2+}/H^{+} antiporters exist at this organelle (Sze et al., 2000; Sanders et al., 2002) to help regulate intracellular Ca^{2+} levels. The work described here provides further evidence that CAX1, a Ca^{2+}/H^{+} antiporter, localizes to the vacuolar membrane in Arabidopsis (Figure 1) and plays a central role in modulating myriad plant responses.

CAX1 Localization

An NRR on CAX1 has been shown to regulate Ca^{2+} transport by the mechanism of N-terminal autoinhibition (Pittman and Hirschi, 2001; Pittman et al., 2002). Here, we demonstrate that a HA-tagged version of CAX1 that lacks the NRR may localize to the tonoplast of transgenic Arabidopsis and tobacco (Figure 1). Using an antibody directed against the NRR, we also demonstrate that full-length CAX1 localizes to the Arabidopsis tonoplast. The Mg^{2+}-shift experiment suggests that CAX1 does not localize to the endoplasmic reticulum; furthermore, chlorophyll levels (a chloroplast marker) peaked in 41 to 43% Suc fractions in the presence or absence of Mg^{2+} (data not shown), indicating that CAX1 is not found at this organelle. However, we still cannot exclude CAX1 localization to the Golgi; thus, such clarification will have to wait for CAX1–green fluorescent protein fusion studies. Future work using CAX1–green fluorescent protein fusions also will be needed to determine if CAX1 is localized differentially on small vacuoles or large central vacuoles

(Paris et al., 1996). For example, CAX1 may be localized to a different vacuolar subtype from that proposed for ACA4 (Geisler et al., 2000).

These expression studies also demonstrate that full-length CAX1 is expressed in Arabidopsis, suggesting that CAX1 is not alternatively spliced to remove the NRR, as is seen with the regulatory domains of some mammalian plasma membrane–type Ca^{2+}-ATPases (Penniston and Enyedi, 1998). Moreover, this finding suggests that the NRR is not a cleavable signal peptide (Darley et al., 2000). In total, these data allow us to conclude unambiguously that the NRR is present on the CAX1 transporter.

Although the vacuole is an important Ca^{2+} store, other organelles, such as the endoplasmic reticulum and the mitochondrion, may be important intracellular Ca^{2+} stores as well (Sanders et al., 2002). Various abiotic stresses induce Ca^{2+} release from different stores (Knight and Knight, 2001). For example, mitochondria are required for Ca^{2+} release in response to anoxia (Subbaiah et al., 1998). Although *cax1* showed increased tolerance to a variety of ionic stresses (see below), there was no observed difference between *cax1* and the wild type for other abiotic stresses, such as temperature and mannitol (data not shown). This result may indicate that the disruption in Ca^{2+} loading into the vacuole may affect only some signaling pathways.

Altered Vacuolar H^{+}-ATPase Activity in the *cax1* Lines

The transport system of the vacuolar membrane includes H^{+} pumps and several secondary active transporters. Two distinct H^{+} pumps, the V-ATPase and the V-PPase, are found on the tonoplast, and each has been well characterized (Barkla and Pantoja, 1996; Drozdowicz and Rea, 2001; Sze et al., 2002). These pumps create an electrochemical gradient of protons across the tonoplast, and this gradient is used as a source of energy for a variety of antiporters. For example, a stoichiometry of three H^{+} to one Ca^{2+} has been estimated for a vacuolar Ca^{2+}/H^{+} antiporter (Blackford et al., 1990). As measured by direct ATP-dependent H^{+}-pumping activity, the *cax1* lines showed an ~40% decrease in V-ATPase activity (Figure 3). Meanwhile, the deregulated *CAX1*-expressing lines showed a 26% increase in V-ATPase activity. Measurements of V-ATPase hydrolytic activity also supported these results (data not shown). These findings suggest that when CAX1 activity is high, V-ATPase activity is increased in response to the enhanced requirement for protons to drive CAX1-mediated Ca^{2+}/H^{+} antiport. In the absence of CAX1, V-ATPase activity is reduced similarly. The changes observed in V-ATPase activity may result from the direct regulation by both transporters whereby CAX1 interacts physically with a V-ATPase subunit to modulate activity; alternatively, the V-ATPase activity may be reduced because of increased consumption of ATP used to drive Ca^{2+}-ATPase activity (Figure 4) (see below).

Potentially, the numerous subtle phenotypes shown in the *cax1-1* and *cax1-2* alleles could be attributable to minor alterations in vacuolar biogenesis (Rojo et al., 2001); however, preliminary studies suggest that this is not the case. For example, *cax1-1* root cells do not exhibit significant alterations in cell and vacuole morphology, as shown by visualization of wild-type and *cax1-1* vacuoles upon staining with a vacuole-loaded fluorescent dye (Emans et al., 2002) and by comparisons of wild-type and *cax1-1* protoplast morphology (data not shown). Furthermore, the alterations in vacuolar transporter expression and activity are specific and do not affect numerous vacuolar proteins. Although there are alterations in V-ATPase and Ca^{2+}-ATPase activity and *CAX3* and *CAX4* expression, there is no significant alteration in V-PPase activity (data not shown) or *AtNHX1* and *CAX2* gene expression (Figure 5). Together, these findings suggest that only a subset of vacuolar transporters are perturbed, and these alterations are not caused by alterations in vacuolar morphology.

CAX1 and the Hierarchy of Vacuolar Ca^{2+} Transporters

In yeast, a null mutant in *VCX1*, the Ca^{2+}/H^{+} antiporter, has no severe consequences on normal yeast growth despite these strains lacking all vacuolar Ca^{2+}/H^{+} antiport activity (Cunningham and Fink, 1996; Miseta et al., 1999). Recently it was demonstrated that a hypertonic shock in yeast can release Ca^{2+} from the vacuole, and resetting this Ca^{2+} spike requires VCX1 but not the vacuolar Ca^{2+}-ATPase PMC1 (Denis and Cyert, 2002). This finding suggests that vacuolar Ca^{2+}/H^{+} transport is important in a subset of Ca^{2+} signal transduction events.

Although additional vacuolar Ca^{2+} sequestration pathways exist in plants, CAX1 contributes substantially to Ca^{2+} homeostasis. RNA analysis demonstrates that *CAX1* is expressed in all tissues (Hirschi, 1999). In the two transposon-insertion mutants of *cax1* reported here, *CAX1* RNA and protein were not detected (Figure 2) and CAX1-mediated Ca^{2+}/H^{+} antiport activity was abolished completely, as demonstrated by the lack of inhibition of antiport activity by a CAX1-specific synthetic peptide (Figure 4C). The two null alleles of *CAX1* have various alterations in plant growth and development (detailed below) and vacuolar Ca^{2+} transport, even though vacuolar Ca^{2+}-ATPase activity was enhanced and *CAX3* and *CAX4* RNA expression was increased (Figures 4 and 5). The enhanced expression of other transporters in the *cax1* alleles is similar to the heightened ferric chelate reductase activity and *IRT2* expression seen in the *irt1-1* iron transport mutant (Vert et al., 2002). However, *irt1-1* has a dramatic phenotype that cannot be compensated for despite upregulation of a homologous transporter. The induction of other putative Ca^{2+} transport systems, through some unknown regulatory network, must try to compensate for the loss of *CAX1*, suggesting the presence of a global mechanism of transcriptional regulation for vacuolar Ca^{2+} transporters. However, as shown by our Ca^{2+} transport

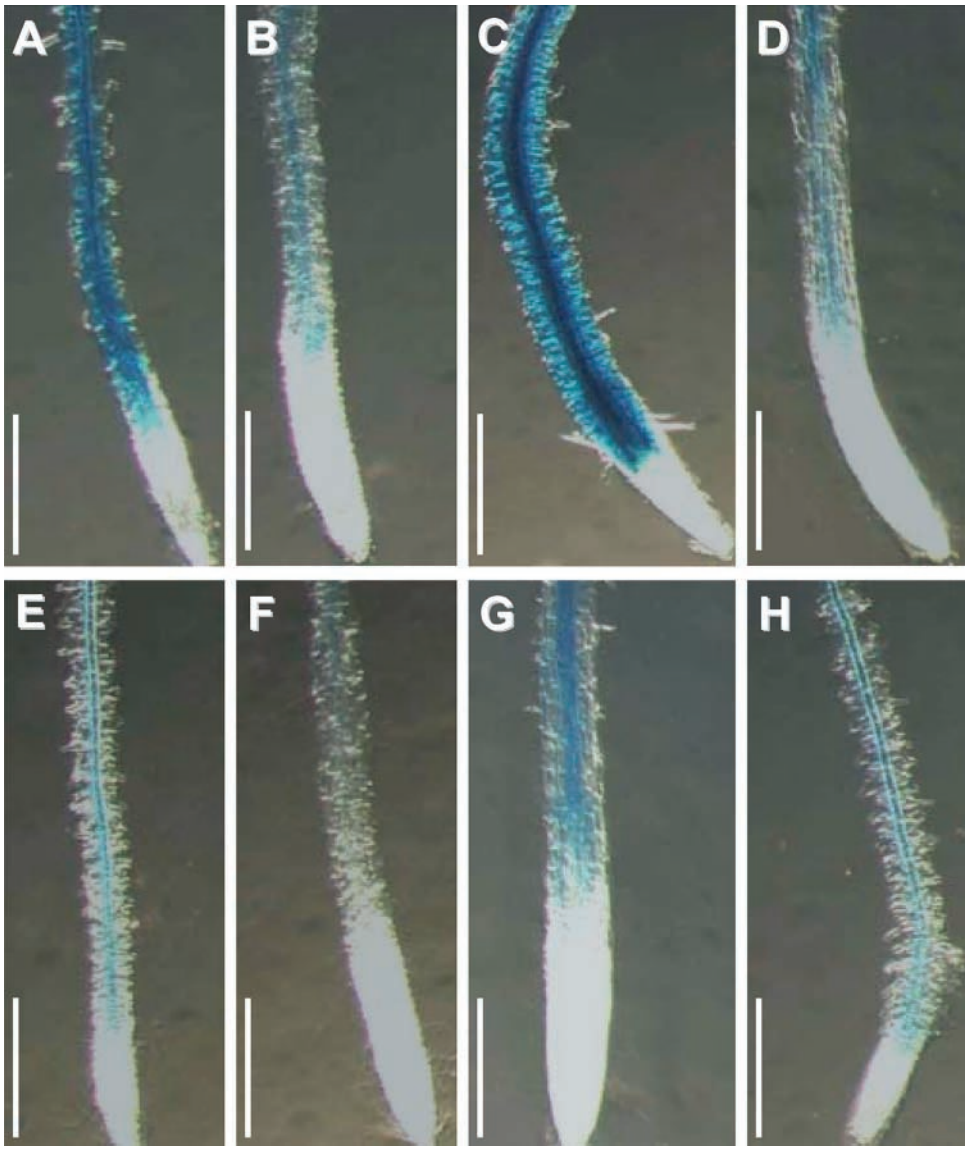

Figure 10. *IAA28*-GUS Expression in Wild-Type and *cax1-1* Plants.

IAA28-GUS wild-type and *cax1-1* seedlings grown under yellow-filtered light on half-strength MS medium for 5 days were transferred onto half-strength MS medium (**[A]** and **[E]**), 10 mM $CaCl_2$ containing half-strength MS medium (**[B]** and **[F]**), or Ca^{2+}-depleted medium (**[C]** and **[G]**) and then grown for another 3 days. Half of the seedlings from half-strength MS medium were treated with 20 μM IAA solution (**[D]** and **[H]**) for 4 h. All seedlings were stained with 1 mM 5-bromo-4-chloro-3-indolyl-β-D-glucuronic acid for 3 h at 37°C. Results from a representative experiment are shown. Approximately 100 F2 progeny were analyzed under each condition in the *cax1-1* lines. The GUS staining shown here correlated with *cax1-1* segregation in all 100 F2 progeny of the *cax1-1* lines analyzed. Bars = 0.5 mm.

data, this compensation is incomplete and resulted in an increase in high-affinity Ca^{2+}-ATPase–mediated Ca^{2+} transport but a net decrease in low-affinity, high-capacity Ca^{2+}/H^+ antiporter–mediated Ca^{2+} transport (Figure 4).

The increased vacuolar Ca^{2+}-ATPase activity (Figure 4B) may be mediated by the increased expression of *ACA4* (Figure 5A). ACA4 is localized only on small vacuoles rather than on the large central vacuole (Geisler et al., 2000). Alternatively, other Ca^{2+}-ATPases on the tonoplast, such as ACA11, which is the closest related transporter to ACA4 (Axelsen and Palmgren, 2001), may be responsible for the transport increases. It is the Ca^{2+}/H^+ antiporter rather than

Ca^{2+}-ATPase that efficiently sequesters Ca^{2+} when cytosolic Ca^{2+} levels are high (Miseta et al., 1999); therefore, an increase in Ca^{2+}-ATPase activity may not be enough to efficiently reduce cytosolic Ca^{2+} in *cax1*.

Although the precise functions of CAX3 and CAX4 remain unknown (Shigaki and Hirschi, 2000; Cheng et al., 2002), the increased expression of these transporters in the *cax1* alleles suggests that they play a role in Ca^{2+} homeostasis. This assumption is strengthened by the lack of induction of the characterized Na^+ and metal antiporters in the *cax1* alleles. These results also suggest that detailed expression profiling of the *cax1* alleles may help identify other genes involved in Ca^{2+} homeostasis. Despite the increased expression of *CAX3* and *CAX4*, the reduction in Ca^{2+}/H^+ transport in roots indicated that no antiport activity in the roots can compensate completely for the loss of *CAX1*. It is possible that a reduced H^+ gradient attributable to decreased V-ATPase activity prevented Ca^{2+}/H^+ antiport by CAX3 and CAX4.

Phenotypes of *cax1* Alleles

Many Arabidopsis knockout mutants fail to display any morphological phenotype, presumably because of functional redundancy (Krysan et al., 1999). *CAX1* is a member of a large multigene family (Mäser et al., 2001) and just one of many Ca^{2+} efflux transporter genes present in Arabidopsis (Sze et al., 2000; Sanders et al., 2002). That we have identified a number of phenotypes, although subtle, for *cax1* highlights its importance in plant growth. Although the knockout mutant of another endomembrane Ca^{2+} transporter, the Ca^{2+}-ATPase ECA1, also showed subtle phenotypes, only a modest reduction in Ca^{2+} transport was observed (Wu et al., 2002), whereas the lack of CAX1 resulted in a significant disruption in Ca^{2+}/H^+ antiport activity.

The *cax1* mutant displayed a significant alteration in flowering time (Figure 8). We have yet to determine the mechanism for this alteration. It is interesting that the Arabidopsis V-ATPase mutant *det3* displays a variety of phenotypes that include reductions in hypocotyl, petiole, and inflorescence stem cell elongation (Schumacher et al., 1999). The *det3* mutant has a 60% reduction in V-ATPase activity, which also is correlated with a reduction in plant height during the reproductive phase. However, the *det3* phenotypes are much more pronounced than those in the *cax1* lines, and at a later age the *cax1* plants are indistinguishable from wild-type plants (data not shown). Currently, it is unclear which of the *det3* phenotypes are attributable directly to a reduction in V-ATPase activity or to secondary effects caused by a reduction in the H^+ gradient. For example, stomatal closure phenotypes of the *det3* mutant attributable to various abiotic stresses have been suggested to be caused by a disruption of vacuolar Ca^{2+}/H^+ antiporter activity that may require energization by the V-ATPase (Allen et al., 2000). The modest 20% difference in V-ATPase activity between the *cax1* lines and the *det3* lines is difficult to reconcile with these dramatic phenotypic differences between the mutants. However, the mutants may differ in spatial and temporal reduction in V-ATPase activity. The cause of the *det3* V-ATPase reduction is known: a reduction in the C-subunit. Additional work is required to determine the mechanism of diminished V-ATPase activity in the *cax1* lines.

Phenotypes of Altered Vacuolar Ca^{2+}/H^+ Antiport: More versus Less

The phenotypes associated with the disruption of *CAX1* can be compared and contrasted with the phenotypes obtained in *CAX1* gain-of-function studies (Hirschi, 1999). A greater than twofold increase in root Ca^{2+} levels was measured in tobacco plants ectopically expressing deregulated *CAX1* (Hirschi, 1999). This alteration in total ion content, presumably causing altered Ca^{2+} partitioning, was associated with the plants being more sensitive to environmental perturbations, such as high levels of Mg^{2+}, K^+, Na^+, and cold. Although the *cax1* alleles did not show altered ion content in any tissue analyzed (data not shown), they did exhibit the opposing stress phenotype: the plants were more tolerant of an array of ion imbalances, including K^+, Na^+ (data not shown), Mg^{2+}, and Mn^{2+} (Figure 6). The growth of the *cax1* alleles in medium containing Mg^{2+} and Mn^{2+} resembles the growth of wild-type plants in medium containing both Mg^{2+} and Ca^{2+} or medium containing Mn^{2+} and Ca^{2+} (data not shown). Exogenous Ca^{2+} can buffer the toxicity of numerous ions in the growth medium (Epstein, 1998). These ion tolerances exhibited by the *cax1* alleles (which are reversible when sCAX1 is expressed) suggest that the *cax1* lines have growth phenotypes that mimic the growth of wild-type plants in the presence of exogenous Ca^{2+}.

However, the modest ion tolerances of the *cax1* alleles are puzzling in the context of the reduced V-ATPase activity (Figure 3). Increased V-PPase activity increases Na^+ tolerance significantly (Gaxiola et al., 2001), so it may follow that reduced V-ATPase activity should reduce ion tolerance dramatically (Gaxiola et al., 2002). As mentioned above, the altered V-ATPase activity found in the *cax1* lines may be conditional, and the V-ATPase actually may be upregulated during these ion perturbations (Dietz et al., 2001). Alternatively, the altered expression of the other transporters (Figure 5) may compensate for the alterations in V-ATPase activity.

As with the ion tolerances, the *cax1* lines were resistant to the inhibition of root elongation by a variety of hormones, particularly auxin (Figure 9). Many abiotic stresses, such as salinity (Knight et al., 1997), and various hormones, such as auxin (Felle, 1988), abscisic acid (Staxén et al., 1999), and gibberellin (Bush and Jones, 1988), stimulate increased cytosolic Ca^{2+}. Ca^{2+} is a central component in many abiotic signaling pathways, and cytosolic Ca^{2+} increase is an early event response (Knight and Knight, 2001). One model for these phenotypes may be that if cytosolic Ca^{2+} increases

above a certain threshold, which can be expected when CAX1 is disrupted, then a response that usually is induced by a stimulus via Ca^{2+} increase may not occur. Thus, in the *cax1* lines, the duration of the cytosolic Ca^{2+} pulse is prolonged, so the response to a particular stimulus, such as auxin, does not occur. Conversely, in the *CAX1*-expressing plants, the duration of the cytosolic Ca^{2+} burst is attenuated and the stress response is heightened. Future studies, particularly Ca^{2+} imaging studies, should be directed at discerning the mechanistic cause of these different stress phenotypes.

Wild-type Arabidopsis displays a Ca^{2+} deficiency response when grown on Ca^{2+}-deplete medium, but *cax1* plants are tolerant of the lack of Ca^{2+} (Figures 6G and 6H). Various organelles, such as the endoplasmic reticulum and the Golgi, require Ca^{2+} to support biological functions (Sanders et al., 2002). The reduction in vacuolar Ca^{2+} sequestration in *cax1* presumably allows some Ca^{2+} to be available for other endomembrane compartments. The importance of Ca^{2+} efflux into other endomembrane compartments has been highlighted in recent studies. For example, a T-DNA mutation in the endoplasmic reticulum Ca^{2+}-ATPase ECA1 caused the growth of the *eca1* plants to be impaired on low-Ca^{2+} medium (Wu et al., 2002).

IAA28 Levels Are Reduced in *cax1*

The *cax1* phenotypes, particularly the alterations in apical dominance and lateral root development, led us to further investigate the relationship between auxin and CAX1. We obtained several promoter–GUS reporter constructs of various auxin-regulated genes and response elements, including the synthetic auxin response element *DR5* (Ulmasov et al., 1997) and *IAA28*, a member of the *Aux*/*IAA* gene family (Rogg et al., 2001). Although we observed no difference in *DR5* expression between *cax1* and the wild type, *IAA28* expression was more interesting. Whereas most *Aux*/*IAA* genes are upregulated by IAA, *IAA28* is downregulated (Rogg et al., 2001) (Figure 10D). However, we observed that the *IAA28* reporter is sensitive to Ca^{2+} perturbations in the medium (Figure 10), with exogenous Ca^{2+} repressing *IAA28* expression. The use of the *IAA28* promoter–GUS construct thus allows us to use another tool to infer the Ca^{2+} status within *cax1* plants. The observation that *IAA28* expression is decreased in *cax1-1* plants on normal medium suggests conditions within the plants that phenocopy the application of high exogenous Ca^{2+}. Furthermore, we found no differences in *IAA28* expression in plants grown in medium containing increased levels of Mn^{2+} and Mg^{2+}, suggesting that this reporter does not respond to general changes in ion homeostasis (data not shown). This finding agrees with the induction of *CAX3* RNA levels in *cax1-1* plants (Figure 5), because in a previous study we have shown *CAX3* induction by exogenous Ca^{2+} (Shigaki and Hirschi, 2000). We believe that these alterations in *IAA28* expression are not mediated by auxin, because *cax1* lines did not display drastic alterations in other auxin-responsive reporters (data not shown) and the lateral root phenotypes displayed by the mutants are not consistent with increased levels of auxin.

Summary

The *cax1* phenotypes reported here are especially noteworthy when one considers that 50% of the Ca^{2+}/H^{+} antiport activity remains at the plant tonoplast (Figure 4B). Despite this residual Ca^{2+}/H^{+} antiport, there is a 36% increase in vacuolar Ca^{2+}-ATPase activity and a 40% reduction in V-ATPase activity. Given the compensatory responses in vacuolar transporters seen in the *cax1* alleles, further analysis of Ca^{2+} sequestration into the plant vacuole will require the creation of multiple CAX mutations to fully attenuate vacuolar Ca^{2+}/H^{+} antiporter activity.

METHODS

Isolation of *CAX1* Knockout Mutants

For the isolation of a mutant carrying a d*Spm* transposon insertion in *CAX1* (ecotype Columbia), pools of genomic DNA representing a population of SLAT lines (Sainsbury Laboratory *Arabidopsis thaliana* Transposants) (Tissier et al., 1999) were screened by PCR using *CAX1*- and d*Spm*-specific primers. Four pairs of primers were used, each pair including a d*Spm*-specific primer (5′-CTTATTTCAGTAAGAGTGTGGGGTTTGG-3′ for the left border of d*Spm* and 5′-GGTGCAGCAAAACCCACACTTTTACTTC-3′ for the right border of d*Spm*) and a *CAX1* gene-specific primer (5′-AAAAAATCAGACCTCCGAGTGATTCAGAA-3′ for the 5′ end of *CAX1* and 5′-CCTTTCTCCATTGTCTCTGCTTTGGAAA-3′ for the 3′ end of *CAX1*). A pool from which a PCR product gave a positive signal after DNA gel blot hybridization with the *CAX1* gene probe was rescreened by PCR using the four pairs of primers. After three rounds of PCR screening, individual plants were identified from the pool. One homozygous and one heterozygous plant carrying the d*Spm* insertion in *CAX1* were isolated. The homozygous plant line was termed *cax1-1*. The location of the d*Spm* insertion was determined by sequencing of the PCR product. Using the same approach, another *cax1* allele carrying a *Ds* transposon insertion in *CAX1* (SGT [Singapore Gene Trap]; *Ds* insertion lines, ecotype Landsberg *erecta*) (Parinov et al., 1999) was isolated from seed pools that were obtained from the ABRC Seed Stock Center (Columbus, OH). The *Ds*-specific primers used in this screening were Ds5′-2 (5′-TCCGTTCGTTTTCGTTTTTTAC-3′ for the 5′ end of *Ds*) and Ds3′-2 (5′-CGATTACCGTATTTATCCCGTTC-3′ for the 3′ end of *Ds*). The homozygous plant line was termed *cax1-2*. Both *cax1* alleles were backcrossed to their parental plants to remove any potential unlinked mutations (Vitart et al., 2001).

Plant Materials and Growth Conditions

Arabidopsis thaliana ecotypes Columbia (Col-0) and Landsberg *erecta* (L*er*) were used in this study. Wild-type and *cax1* mutant seeds were surface-sterilized, germinated, and grown on half-

strength MS medium (Murashige and Skoog, 1962) containing 0.5% Suc solidified with 0.8% agar. All plates were sealed with paper surgical tape (Tenderskin; The Kendall Company, Mansfield, MA) and incubated at 22°C under continuous cool-fluorescent illumination for various intervals under various environmental conditions. For the ion sensitivity assays, 5-day-old wild-type and *cax1* seedlings grown under normal conditions were transferred onto half-strength MS medium and the identical medium supplemented with various metal ions (as described in the legend to Figure 6) and grown for 5 additional days. To make the medium deficient in Ca^{2+}, we deleted the $CaCl_2$ from the nutrient solution (Hirschi, 1999).

To examine root growth, surface-sterilized seeds were plated on half-strength MS medium and grown for 10 days under standard conditions. The lengths of the primary roots were measured. The numbers and total lengths of lateral roots were examined with a dissecting microscope. A lateral root was scored if a visible primordium was formed, even if it had not yet emerged from the primary root (Rogg et al., 2001).

For hormone sensitivity assays, surface-sterilized wild-type and *cax1* seeds were plated side by side on standard medium and medium with various concentrations of phytohormones (Rogg et al., 2001). All phytohormones were purchased from Sigma (St. Louis, MO). After 10 days of growth at 22°C under yellow-filtered light, the lengths of the primary roots were measured. Root elongation inhibition was calculated as the percentage of primary root growth of seedlings on supplemented medium versus those on standard medium.

To examine the morphological phenotypes of mature wild-type and *cax1* plants, seeds were sown in artificial soil (Metromix 200; Scotts, Marysville, OH), kept at 4°C for 2 days to synchronize germination, and then grown at 24°C under continuous light. Plants were observed and measured once per week from 3 weeks after germination until 6 weeks of age. All photographs were taken using a Nikon digital camera (Coolpix 995; Nikon Corp., Tokyo, Japan).

Plasmid DNA Constructs and Plant Transformation

The deregulated form of *CAX1* (*sCAX1*) was cloned previously in a yeast suppression screen (Hirschi et al., 1996). The triple hemagglutinin (HA) epitope–tagged *sCAX1* (*HA-sCAX1*) was constructed as described previously (Shigaki et al., 2001). Both constructs were subcloned into the plant expression vector pBin19 (BD Bioscience Clontech, Palo Alto, CA), which contained the 35S promoter fragment of *Cauliflower mosaic virus* (Hull et al., 2000). The recombinant plasmids or vector controls were transformed into *Agrobacterium tumefaciens* GV3101 (Sambrook et al., 1989). These strains were used to transform various lines of Arabidopsis using the floral dip method (Clough and Bent, 1998) or tobacco (*Nicotiana tabacum* cv BY-2) suspension cells according to published methods (Matsuoka and Nakamura, 1991). For Arabidopsis transformation, T1 seeds were screened on the selection medium and resistant seedlings were transferred to soil, and T2 seeds were harvested. Homozygous lines were selected by examining the kanamycin resistance of T2 seedlings.

Preparation of Membrane Vesicles, Ca^{2+} Uptake, and V-ATPase Activity

For the measurement of Ca^{2+} uptake, vacuole-enriched membrane vesicles were prepared from root tissue obtained from 4-week-old Col-0 and *cax1-1* mutant plants cultured in 1 × Gamborg's B5 medium (Invitrogen, Carlsbad, CA) and pretreated with 100 mM $CaCl_2$ for 18 h before harvest. All membrane isolation steps were conducted at 4°C. Tissue was homogenized with a mortar and pestle in 4 mL/g fresh weight of homogenization solution containing 0.5 M sorbitol, 50 mM 3-(*N*-morpholino)-propanesulfonic acid–KOH, pH 7.6, 5 mM EDTA, 5 mM EGTA, 1.5% polyvinylpyrrolidone 40,000, 0.5% BSA, 1 mM phenylmethylsulfonyl fluoride (PMSF), and 1 mM DTT. The homogenate was filtered through four layers of cheesecloth and then centrifuged at 12,000*g* for 10 min. The supernatant was diluted in 0.3 M sorbitol, 10% glycerol, 2 mM Tris-Mes, pH 7.6, 1 mM PMSF, and 1 mM DTT and then centrifuged at 120,000*g* for 45 min. The microsomal pellet was resuspended in 15% (w/w) Suc solution (containing 10 mM Tris-Mes, pH 7.6, 1 mM EGTA, 25 mM KCl, 1.1 M glycerol, 0.2% BSA, 2 mM DTT, 1 mM PMSF, and 1 mg/L leupeptin), layered onto a 35% (w/w) Suc solution, and then centrifuged at 150,000*g* for 30 min. Endomembrane-enriched vesicles were collected at the interface and diluted in 5 mM Tris-Mes, pH 7.6, 0.3 M sorbitol, 1 mM EGTA, 0.1 M KCl, 1 mM DTT, 1 mM PMSF, and 1 mg/L leupeptin. The membranes were centrifuged at 150,000*g* for 30 min, resuspended in 0.3 M sorbitol, 5 mM Tris-Mes, pH 7.6, 1 mM PMSF, and 1 mM DTT, and stored in liquid N_2 until use.

For the measurement of V-ATPase activity, microsomal membranes were isolated according to Barkla et al. (1999) from root tissue obtained from 4-week-old wild-type plants (Col-0 and L*er*), *cax1* mutant plants (*cax1-1* and *cax1-2*), and the transgenic line *cax1-1*:*CAX1*. All plants were cultured in 1 × Gamborg's B5 medium (Invitrogen). Microsomal membranes then were subjected to Suc density gradient centrifugation, and purified tonoplast vesicles were collected according to Apse et al. (1999). Membranes were frozen directly in liquid N_2 and stored at −80°C. Those used for quinacrine fluorescence measurements were subjected to only a single freeze/thaw cycle, because additional cycles increased the leakiness of the vesicles.

Time-dependent Ca^{2+} uptake into vacuolar membrane vesicles by Ca^{2+}/H^+ antiport and calmodulin-stimulated Ca^{2+}-ATPase activity was measured using the filtration method (Pittman and Hirschi, 2001). Membrane vesicles were incubated in a reaction mixture containing 0.3 M sorbitol, 5 mM Tris-Mes, pH 7.6, 25 mM KCl, 0.1 mM NaN_3, and 1 mM Mg^{2+}-ATP. Uptake was initiated by the addition of 10 μM $^{45}CaCl_2$ (6 mCi/mL; American Radiolabeled Chemicals, St. Louis, MO). At the times indicated in Figure 4, 70-μL aliquots of the reaction mixture were filtered through premoistened 0.45-μm (pore size) cellulose acetate GS-type filters (Millipore, Bedford, MA) and washed with 1 mL of ice-cold wash buffer containing 0.3 M sorbitol, 5 mM Tris-Mes, pH 7.6, 25 mM KCl, and 1 mM $CaCl_2$. The filters were air-dried, and radioactivity was determined by liquid scintillation counting. For some experiments, Ca^{2+} uptake was measured in the presence of 0.2 mM sodium orthovanadate, 5 μM carbonyl cyanide *p*-(trifluoromethoxy)phenylhydrazone, or 0.5 μM bovine brain calmodulin (Sigma).

V-ATPase H^+ transport activity was measured by the fluorescence quenching of quinacrine (6-chloro-9-{[4-(diethylamino)-1-methylbutyl]amino}-2-methoxyacridine dihydrochloride) by monitoring the formation and dissipation of inside-acid pH gradients across tonoplast vesicles, as described previously (Barkla et al., 1999). Fluorescence quenching was monitored in a thermostated cell at 25°C using a fluorescence spectrometer (model LS-50; Perkin-Elmer) at excitation and emission wavelengths of 427 and 495 nm, respectively, both with a slit width of 5 nm. As shown by Bennett and Spanswick (1983), the rate of fluorescence quenching is directly proportional to proton flux; thus, initial rates of fluorescence quenching represent initial rates of proton transport.

Preparation of Protoplasts and Visualization of Dye-Loaded Vacuoles

To generate protoplasts, 2-week-old wild-type and *cax1* mutant plants cultured in 1 × Gamborg's B5 medium (Invitrogen) were harvested and incubated in culture medium containing 400 mM mannitol, 1% cellulose R10, and 0.25% Macerozyme R10 (Karlan, Inc., Santa Rosa, CA) for 4 h at 26°C with gentle shaking (Geisler et al., 2000). Protoplasts were filtered through two layers of cheesecloth and chilled on ice before use.

To examine the morphology of the vacuoles (central vacuoles and small vacuoles) in both protoplasts and intact root tissue cells of wild-type and *cax1* mutant plants, a highly polar dye (Alexa 568 hydrazide, a fluid-phase vacuolar maker; Molecular Probes, Eugene, OR) was used to label the cells and protoplasts according to a published procedure (Emans et al., 2002) with minor modification. The root tissue (short cuttings of roots) and the protoplasts in the culture medium were chilled on ice for 30 min, supplemented with 100 μM Alexa 568 hydrazide (50 mM), and then incubated at 26°C for 4 h with gentle shaking. The cells or root tissues were washed three times with the ice-cold culture medium and imaged using an epifluorescence Axiophot microscope (Carl Zeiss, Inc., Thornwood, NY) equipped with a digital detection system (DEI-750D CE Digital Output, model S60675/S60674 PAL/NTSC; Optronics, Goleta, CA) using a 600-nm barrier filter.

RNA Gel Blot Analysis

RNA gel blot analysis was performed as described previously (Hirschi, 1999). Three-week-old Arabidopsis wild-type (Col-0 and L*er*) and *cax1* mutant plants were harvested and treated with water (as a control), 10 mM $CaCl_2$, or 80 mM NaCl for 16 h. Total RNA was extracted, blotted, and hybridized with ^{32}P-labeled gene-specific probes. Hybridization results were quantified with a PhosphorImager SI and ImageQuant software (Molecular Dynamics, Sunnyvale, CA).

Membrane Fractionation of HA-sCAX1–Expressing Arabidopsis and Tobacco BY-2 Cells

Microsomal membranes were prepared from HA-sCAX1–expressing Arabidopsis seedlings or tobacco BY-2 suspension cells as described previously (Cheng et al., 2002). Wild-type and HA-sCAX1 transgenic Arabidopsis grown in 1 × Gamborg's B5 medium were homogenized, and microsomes were prepared as described above. For some preparations, wild-type Arabidopsis also was homogenized with the addition of 5 mM $MgCl_2$ in the homogenization buffer. Microsomes (0.5 mL) were layered onto a 15 to 50% (w/w) Suc gradient containing 10 mM Tris-Mes, pH 7.6, 1 mM EGTA, 25 mM KCl, 1.1 M glycerol, 0.2% BSA, 2 mM DTT, 1 mM PMSF, and 1 mg/L leupeptin and centrifuged at 150,000*g* for 16 h. For the Mg^{2+}-shift Suc gradients, 5 mM $MgCl_2$ was added to the centrifugation and Suc gradient buffers. Fractions (0.5 mL) were collected and stored at −80°C until use.

Preparation of the CAX1 Antibody and Protein Gel Blot Analysis

An anti-peptide antibody was raised against a synthetic peptide (CAX1-NRR) that corresponds to the first 36 amino acids of full-length CAX1 (Pittman et al., 2002). The antibody was raised (Alpha Diagnostic International, San Antonio, TX) in rabbits by injection of the peptide conjugated to keyhole limpet hemocyanin and then affinity purified against the CAX1-NRR peptide using Sepharose column chromatography.

Immunoblot analysis was performed as described previously (Pittman and Hirschi, 2001). The HA epitope and the membrane marker proteins were detected as described previously (Cheng et al., 2002). Monoclonal antibodies against HA (Berkely Antibody Co., Richmond, CA) and the plant endoplasmic reticulum luminal protein (BiP; StressGen Biotechnologies, Victoria, British Columbia, Canada) were used at dilutions of 1:1000 and 1:1500, respectively. Polyclonal antibodies against the mung bean (*Vigna radiata*) vacuolar pyrophosphatase (V-PPase) and radish plasma membrane aquaporin (PAQ1) were used at a dilution of 1:1000 (Nakanishi et al., 2001; Suga et al., 2001). The CAX1-NRR anti-peptide antibody was used at a dilution of 1:2000.

Reporter Gene Assay

To determine whether the knockout of the *CAX1* gene perturbed the auxin signaling pathway, we performed backcrossing of *cax1-1* plants with two reporting lines, *DR5*-GUS (Ulmasov et al., 1997) and *IAA28*-GUS (Rogg et al., 2001). F2 plants were used to examine GUS expression under different treatments. Histochemical analysis of GUS expression was performed as described previously (Oono et al., 1998) with minor modifications. Five-day-old seedlings grown under yellow-filtered light were transferred onto standard medium with or without 10 mM $CaCl_2$ and Ca^{2+}-depleted medium and then grown for an additional 3 days. The yellow-filtered light decreased the fluence of light (approximately twofold) and slowed the photochemical breakdown of indolic compounds (Rogg et al., 2001). Half of the seedlings from the standard medium were treated with 20 μM indoleacetic acid for 4 h before being examined for GUS expression. The seedlings were rinsed three times with staining buffer lacking 5-bromo-4-chloro-3-indolyl-β-D-glucuronide [50 mM sodium phosphate, pH 7.2, 0.5 mM $K_4Fe(CN)_6$, 0.5 mM $K_3Fe(CN)_6$] and then incubated for 3 h at 37°C in staining buffer containing 1 mM 5-bromo-4-chloro-3-indolyl-β-D-glucuronic acid. To clear chlorophyll from the green tissues, the stained seedlings were incubated in 70% ethanol overnight at 4°C and then kept in 95% ethanol. GUS staining patterns were recorded using a Zeiss Axiophot microscope, and images were processed using Adobe Photoshop software (version 6.0; Adobe Systems, San Jose, CA).

Upon request, all novel materials described in this article will be made available in a timely manner for noncommercial research purposes.

ACKNOWLEDGMENTS

We thank Masayoshi Maeshima for the V-PPase peptide and PAQ1 peptide antibodies and Bonnie Bartel for *IAA28*-GUS seeds. We acknowledge Karen Hirschi for the use of the dissecting microscope. We also thank Roberto Gaxiola, Sherry LeClere, and Paul Nakata for their comments. This work was supported by the U.S. Department of Agriculture/Agricultural Research Service under Cooperative Agreement 58-6250-6001 and by National Institutes of Health Grants CHRC 5 P30 and 1R01 GM57427.

Received August 30, 2002; accepted November 14, 2002.

REFERENCES

Abel, S., Nguyen, M.D., and Theologis, A. (1995). The *PS-IAA4/5*-like family of early auxin-inducible mRNAs in *Arabidopsis thaliana*. J. Mol. Biol. **251,** 533–549.

Allen, G.J., Chu, S.P., Schumacher, K., Shimazaki, C.T., Vafeados, D., Kemper, A., Hawke, S.K., Tallman, G., Tsien, R.Y., Harper, J.F., Chory, J., and Schroeder, J.I. (2000). Alteration of stimulus-specific guard cell calcium oscillations and stomatal closing in *Arabidopsis det3* mutant. Science **289,** 2338–2342.

Allen, G.J., Muir, S.R., and Sanders, D. (1995). Release of Ca^{2+} from individual plant vacuoles by both $InsP_3$ and cyclic ADP-ribose. Science **268,** 735–737.

Apse, M.P., Aharon, G.S., Snedden, W.A., and Blumwald, E. (1999). Salt tolerance conferred by overexpression of a vacuolar Na^+/H^+ antiport in *Arabidopsis*. Science **285,** 1256–1258.

Axelsen, K.B., and Palmgren, M.G. (2001). Inventory of the superfamily of P-type ion pumps in Arabidopsis. Plant Physiol. **126,** 696–706.

Barbier-Brygoo, H., Gaymard, F., Rolland, N., and Joyard, J. (2001). Strategies to identify transport systems in plants. Trends Plant Sci. **6,** 577–585.

Barkla, B.J., and Pantoja, O. (1996). Physiology of ion transport across the tonoplast of higher plants. Annu. Rev. Plant Physiol. Plant Mol. Biol. **47,** 159–183.

Barkla, B.J., Vera-Estrella, R., Maldonado-Gamma, M., and Pantoja, O. (1999). Abscisic acid induction of vacuolar H^+-ATPase activity in *Mesembryanthemum crystallinum* is developmentally regulated. Plant Physiol. **120,** 811–819.

Bennett, A.B., and Spanswick, R.M. (1983). Optical measurements of ΔpH and $\Delta\Psi$ in corn root membrane vesicles: Kinetic analysis of Cl^- effects of proton-translocating ATPases. J. Membr. Biol. **71,** 95–107.

Blackford, S., Rea, P.A., and Sanders, D. (1990). Voltage sensitivity of H^+/Ca^{2+} antiport in higher plant tonoplast suggests a role in vacuolar calcium accumulation. J. Biol. Chem. **265,** 9617–9620.

Bush, D.S., and Jones, R.L. (1988). Cytoplasmic calcium and a-amylase secretion from barley aleurone protoplasts. Eur. J. Cell Biol. **46,** 466–469.

Cheng, N.-H., Pittman, J.K., Shigaki, T., and Hirschi, K.D. (2002). Characterization of CAX4: An Arabidopsis H^+/cation antiporter. Plant Physiol. **128,** 1245–1254.

Clough, S.J., and Bent, A.F. (1998). Floral dip: A simplified method for *Agrobacterium*-mediated transformation of *Arabidopsis thaliana*. Plant J. **16,** 735–743.

Cunningham, K.W., and Fink, G.R. (1996). Calcineurin inhibits *VCX1*-dependent H^+/Ca^{2+} exchange and induces Ca^{2+}-ATPases in *Saccharomyces cerevisiae*. Mol. Cell. Biol. **16,** 2226–2237.

Darley, C.P., van Wuytswinkel, O.C.M., van der Woude, K., Mager, W.H., and De Boer, A.H. (2000). *Arabidopsis thaliana* and *Saccharomyces cerevisiae NHX1* genes encode amiloride sensitive electroneutral Na^+/H^+ exchangers. Biochem. J. **351,** 241–249.

Denis, V., and Cyert, M.S. (2002). Internal Ca^{2+} release in yeast is triggered by hypertonic shock and mediated by a TRP channel homologue. J. Cell Biol. **156,** 29–34.

Dietz, K.J., Tavakoli, N., Kluge, C., Mimura, T., Sharma, S.S., Harris, G.C., Chardonnens, A.N., and Golldack, D. (2001). Significance of the V-type ATPase for the adaptation to stressful growth conditions and its regulation on the molecular and biochemical level. J. Exp. Bot. **52,** 1969–1980.

Drozdowicz, Y.M., and Rea, P.A. (2001). Vacuolar H^+-pyrophosphatases: From the evolutionary backwaters into the mainstream. Trends Plant Sci. **6,** 206–211.

Emans, N., Zimmermann, S., and Fischer, R. (2002). Uptake of a fluorescent marker in plant cells is sensitive to brefeldin A and wortmannin. Plant Cell **14,** 71–86.

Epstein, E. (1998). How calcium enhances plant salt tolerance. Science **280,** 1906–1907.

Felle, H. (1988). Auxin causes oscillations of cytosolic free calcium in *Zea mays* coleoptiles. Planta **174,** 495–499.

Gaxiola, R.A., Fink, G.R., and Hirschi, K.D. (2002). Genetic manipulation of vacuolar proton pumps and transporters. Plant Physiol. **129,** 967–973.

Gaxiola, R.A., Li, J., Undurraga, S., Dang, L.M., Allen, G.J., Alper, S.L., and Fink, G.R. (2001). Drought- and salt-tolerant plants result from overexpression of the AVP1 H^+-pump. Proc. Natl. Acad. Sci. USA **98,** 11444–11449.

Gaxiola, R.A., Rao, R., Sherman, A., Grisafi, P., Alper, S.L., and Fink, G.R. (1999). The *Arabidopsis thaliana* proton transporters, AtNhx1 and Avp1, can function in cation detoxification in yeast. Proc. Natl. Acad. Sci. USA **96,** 1480–1485.

Geisler, M., Frangne, N., Gomes, E., Martinoia, E., and Palmgren, M.G. (2000). The *ACA4* gene of Arabidopsis encodes a vacuolar membrane calcium pump that improves salt tolerance in yeast. Plant Physiol. **124,** 1814–1827.

Hasenstein, K.H., and Evans, M.L. (1988). Effects of cations on hormone transport in primary roots of *Zea mays*. Plant Physiol. **86,** 890–894.

Hirschi, K. (2001). Vacuolar H^+/Ca^{2+} transport: Who's directing the traffic? Trends Plant Sci. **6,** 100–104.

Hirschi, K.D. (1999). Expression of *Arabidopsis CAX1* in tobacco: Altered calcium homeostasis and increased stress sensitivity. Plant Cell **11,** 2113–2122.

Hirschi, K.D., Korenkov, V., Wilganowski, N., and Wagner, G. (2000). Expression of *Arabidopsis CAX2* in tobacco: Altered metal accumulation and increased manganese tolerance. Plant Physiol. **124,** 125–134.

Hirschi, K.D., Zhen, R., Cunningham, K.W., Rea, P.A., and Fink, G.R. (1996). CAX1, an H^+/Ca^{2+} antiporter from *Arabidopsis*. Proc. Natl. Acad. Sci. USA **93,** 8782–8786.

Hull, A., Vij, R., and Celenza, J.L. (2000). Arabidopsis cytochrome P450s that catalyze the first step of tryptophan-dependent indole-3-acetic acid biosynthesis. Proc. Natl. Acad. Sci. USA **97,** 2379–2384.

Knight, H., and Knight, M.R. (2001). Abiotic stress signaling pathways: Specificity and cross-talk. Trends Plant Sci. **6,** 262–267.

Knight, H., Trewavas, A.J., and Knight, M.R. (1997). Calcium signaling in *Arabidopsis thaliana* responding to drought and salinity. Plant J. **12,** 1067–1078.

Krysan, P.J., Young, J.C., and Sussman, M.R. (1999). T-DNA as an insertional mutagen in Arabidopsis. Plant Cell **11,** 2283–2290.

Krysan, P.J., Young, J.C., Tax, F., and Sussman, M.R. (1996). Identification of transferred DNA insertions within *Arabidopsis* genes involved in signal transduction and ion transport. Proc. Natl. Acad. Sci. USA **93,** 8145–8150.

Luan, S., Kudla, J., Gruissem, W., and Schreiber, S.L. (1996). Molecular characterization of a FKBP-type immunophilin from higher plants. Proc. Natl. Acad. Sci. USA **93,** 6964–6969.

Marty, F. (1999). Plant vacuoles. Plant Cell **11,** 587–599.

Mäser, P., et al. (2001). Phylogenetic relationships within cation-transporter families of *Arabidopsis thaliana*. Plant Physiol. **126,** 1646–1667.

Matsuoka, K., and Nakamura, K. (1991). Properties of a precursor to a plant vacuolar protein required for vacuolar targeting. Proc. Natl. Acad. Sci. USA **88,** 834–838.

McKinney, E.C., Ali, N., Traut, A., Friedmann, K.A., Belostotsky, D.A., McDowell, J.M., and Meagher, R.B. (1995). Sequence-based identification of T-DNA insertion mutations in *Arabidopsis* actin mutants act2-1 and act4-1. Plant J. **8,** 613–622.

Miseta, A., Kellermayer, R., Aiello, D.P., Fu, L., and Bedwell, D.M. (1999). The vacuolar Ca^{2+}/H^{+} exchanger Vcx1p/Hum1p tightly controls cytosolic Ca^{2+} levels in *S. cerevisiae*. FEBS Lett. **451,** 132–136.

Murashige, T., and Skoog, F. (1962). A revised medium for rapid growth and bioassays with tobacco tissue culture. Physiol. Plant. **15,** 473–497.

Nakanishi, Y., Saijo, T., Wada, Y., and Maeshima, M. (2001). Mutagenic analysis of functional residues in putative substrate-binding site and acidic domains of vacuolar H^{+}-pyrophosphatase. J. Biol. Chem. **276,** 7654–7660.

Oono, Y., Chen, Q.G., Overvoorde, P.J., Kohler, C., and Theologis, A. (1998). *age* mutants of Arabidopsis exhibit altered auxin-regulated gene expression. Plant Cell **10,** 1649–1662.

Palmgren, M.G. (2001). Plant plasma membrane H^{+}-ATPases: Powerhouses for nutrient uptake. Annu. Rev. Plant Physiol. Plant Mol. Biol. **52,** 817–845.

Parinov, S., Sevugan, M., Ye, D., Yang, W., Kumaran, M., and Sundaresan, V. (1999). Analysis of flanking sequences from *Dissociation* insertion lines: A database for reverse genetics in Arabidopsis. Plant Cell **11,** 2263–2270.

Paris, N., Stanley, M., Jones, R.L., and Rogers, J.C. (1996). Plant cells contain two functionally distinct vacuolar compartments. Cell **85,** 563–572.

Penniston, J.T., and Enyedi, A. (1998). Modulation of the plasma membrane Ca^{2+}/H^{+} pump. J. Membr. Biol. **165,** 101–109.

Pittman, J.K., and Hirschi, K.D. (2001). Regulation of CAX1, an Arabidopsis Ca^{2+}/H^{+} antiporter: Identification of an N-terminal autoinhibitory domain. Plant Physiol. **127,** 1020–1029.

Pittman, J.K., Shigaki, T., Cheng, N.-H., and Hirschi, K.D. (2002). Mechanism of N-terminal autoinhibition in the *Arabidopsis* Ca^{2+}/H^{+} antiporter CAX1. J. Biol. Chem. **277,** 26452–26459.

Rogg, L.E., Lasswell, J., and Bartel, B. (2001). A gain-of-function mutation in *IAA28* suppresses lateral root development. Plant Cell **13,** 465–480.

Rojo, E., Gillmor, C.S., Kovaleva, V., Somerville, C.R., and Raikhel, N.V. (2001). VACUOLELESS1 is an essential gene required for vacuole formation and morphogenesis in *Arabidopsis*. Dev. Cell **1,** 303–310.

Sambrook, J., Fritsch, E.F., and Maniatis, T. (1989). Molecular Cloning: A Laboratory Manual. (Cold Spring Harbor, NY: Cold Spring Harbor Laboratory Press).

Sanders, D., Brownlee, C., and Harper, J.F. (1999). Communicating with calcium. Plant Cell **11,** 691–706.

Sanders, D., Pelloux, J., Brownlee, C., and Harper, J.F. (2002). Calcium at the crossroads of signaling. Plant Cell **14** (suppl.), S401–S417.

Schumacher, K., Vafeados, D., McCarthy, M., Sze, H., Wilkins, T., and Chory, J. (1999). The *Arabidopsis det3* mutant reveals a central role for the vacuolar H^{+}-ATPase in plant growth and development. Genes Dev. **13,** 3259–3270.

Schumaker, K.S., and Sze, H. (1987). Inositol 1,4,5-trisphosphate releases Ca^{2+} from vacuolar membrane vesicles of oat roots. J. Biol. Chem. **262,** 3944–3946.

Shaul, O., Hilgemann, D.W., de-Almeida-Engler, J., Van Montagu, M., Inzé, D., and Galili, G. (1999). Cloning and characterization of a novel Mg^{2+}/H^{+} exchanger. EMBO J. **18,** 3973–3980.

Shigaki, T., Cheng, N.-H., Pittman, J.K., and Hirschi, K. (2001). Structural determinants of Ca^{2+} transport in the *Arabidopsis* H^{+}/Ca^{2+} antiporter CAX1. J. Biol. Chem. **276,** 43152–43159.

Shigaki, T., and Hirschi, K.D. (2000). Cloning and characterization of *CAX*-like genes in plants: Implications for functional diversity. Gene **257,** 291–298.

Staxén, I., Pical, C., Montgomery, L.T., Gray, J.E., Hetherington, A.M., and McAinsh, M.R. (1999). Abscisic acid induces oscillations in guard-cell cytosolic free calcium that involve phosphoinositide-specific phospholipase C. Proc. Natl. Acad. Sci. USA **96,** 1779–1784.

Subbaiah, C.C., Bush, D.S., and Sachs, M.M. (1998). Mitochondrial contribution to the anoxic Ca^{2+} signal in maize suspension cultured cells. Plant Physiol. **118,** 759–771.

Suga, S.S., Imagawa, S., and Maeshima, M. (2001). Specificity of the accumulation of mRNAs and proteins of the plasma membrane and tonoplast aquaporins in radish organs. Planta **212,** 294–304.

Sze, H., Li, X., and Palmgren, M.G. (1999). Energization of plant cell membranes by H^{+}-pumping ATPases: Regulation and biosynthesis. Plant Cell **11,** 677–689.

Sze, H., Liang, F., Hwang, I., Curran, A.C., and Harper, J. (2000). Diversity and regulation of Ca^{2+} pumps: Insights from expression in yeast. Annu. Rev. Plant Physiol. Plant Mol. Biol. **51,** 433–462.

Sze, H., Schumacher, K., Müller, M.L., Padmanaban, S., and Taiz, L. (2002). A simple nomenclature for a complex proton pump: VHA genes encode the vacuolar H^{+}-ATPase. Trends Plant Sci. **7,** 157–161.

Tissier, A., Marillonnet, S., Klimyuk, V., Patel, K., Torres, M.A., Murphy, G.P., and Jones, J.D.G. (1999). Multiple independent defective *Suppressor-mutator* transposon insertions in Arabidopsis: A tool for functional genomics. Plant Cell **11,** 1841–1852.

Ueoka-Nakanishi, H., Tsuchiya, T., Sasaki, M., Nakanishi, Y., Cunningham, K.W., and Maeshima, M. (2000). Functional expression of mung bean Ca^{2+}/H^{+} antiporter in yeast and its intracellular localization in the hypocotyl and tobacco cells. Eur. J. Biochem. **267,** 3090–3098.

Ulmasov, T., Murfett, J., Hagen, G., and Guilfoyle, T.J. (1997). Aux/IAA proteins repress expression of reporter genes containing natural and highly active synthetic auxin response elements. Plant Cell **9,** 1963–1971.

Vert, G., Grotz, N., Dedaldechamp, F., Gaymard, F., Guerinot, M.L., Brait, J.-F., and Curie, C. (2002). IRT1, an Arabidopsis transporter essential for iron uptake from the soil and for plant growth. Plant Cell **14,** 1223–1233.

Vitart, V., Baxter, I., Doerner, P., and Harper, J.F. (2001). Evidence for a role in growth and salt resistance of a plasma membrane H^{+}-ATPase in the root endodermis. Plant J. **27,** 191–201.

Wu, Z., Liang, F., Hong, B., Young, J.C., Sussman, M.R., Harper, J.F., and Sze, H. (2002). An ER-bound Ca^{2+}/Mn^{2+} pump, ECA1, supports plant growth and confers tolerance to Mn^{2+} stress. Plant Physiol. **130,** 128–137.